SMC-TR-03-06

AEROSPACE REPORT NO.
TR-2003(3397)-1

Aerodynamic Disturbances on Spacecraft in Free-Molecular Flow

17 October 2002

Prepared by

J. A. STORCH
Vehicle Systems Division

Prepared for

SPACE AND MISSILE SYSTEMS CENTER
AIR FORCE SPACE COMMAND
2430 E. El Segundo Boulevard
Los Angeles Air Force Base, CA 90245

National Systems Group

THE AEROSPACE CORPORATION
El Segundo, California

This report was submitted by The Aerospace Corporation, El Segundo, CA 90245-4691, under Contract No. F04701-00-C-0009 with the Space and Missile Systems Center, 2430 E. El Segundo Blvd., Los Angeles Air Force Base, CA 90245. It was reviewed and approved for The Aerospace Corporation by R. J. Skrinska, Principal Director, Guidance and Control Subdivision; and A. T. Pritt, Systems Director, National Systems Group. Michael Zambrana was the project officer.

This report has been reviewed by the Public Affairs Office (PAS) and is releasable to the National Technical Information Service (NTIS). At NTIS, it will be available to the general public, including foreign nationals.

This technical report has been reviewed and is approved for publication. Publication of this report does not constitute Air Force approval of the report's findings or conclusions. It is published only for the exchange and stimulation of ideas.

Michael Zambrana
SMC/AXE

REPORT DOCUMENTATION PAGE

Form Approved
OMB No. 0704-0188

1. REPORT DATE (*DD-MM-YYYY*)	2. REPORT TYPE	3. DATES COVERED *(From - To)*
17-10-2002		

4. TITLE AND SUBTITLE

Aerodynamic Disturbances on Spacecraft in Free-Molecular Flow

5a. CONTRACT NUMBER
F04701-00-C-0009

5b. GRANT NUMBER

5c. PROGRAM ELEMENT NUMBER

6. AUTHOR(S)

Joel A. Storch

5d. PROJECT NUMBER

5e. TASK NUMBER

5f. WORK UNIT NUMBER

7. PERFORMING ORGANIZATION NAME(S) AND ADDRESS(ES)

The Aerospace Corporation
Vehicle Systems Division
El Segundo, CA 90245-4691

8. PERFORMING ORGANIZATION REPORT NUMBER

TR-2003(3397)-1

9. SPONSORING / MONITORING AGENCY NAME(S) AND ADDRESS(ES)

Space and Missile Systems Center
Air Force Space Command
2450 E. El Segundo Blvd.
Los Angeles Air Force Base, CA 90245

10. SPONSOR/MONITOR'S ACRONYM(S)
SMC

11. SPONSOR/MONITOR'S REPORT NUMBER(S)
SMC-TR-03-06

12. DISTRIBUTION/AVAILABILITY STATEMENT

Approved for public release; distribution unlimited.

13. SUPPLEMENTARY NOTES

14. ABSTRACT

This report presents a thorough development of the aerodynamic forces and moments exerted on spacecraft at altitudes where the atmosphere is best described by free molecular flow theory. The gas-surface interaction model is based upon a combination of specular and diffuse reflection as characterized by normal and tangential momentum accommodation coefficients, while the random thermal motion of the atmosphere is described by the Maxwell-Boltzmann distribution law. In the case of non-rotating bodies of arbitrary shape, general expressions in the form of surface integrals are given for the aerodynamic force and moment. Complications due to spin are investigated for the class of axisymmetric bodies rotating about their axis of symmetry but with arbitrary orientation relative to the incident molecular flow. For several simple geometric shapes, the quadratures are performed analytically, and closed-form expressions are given for the aerodynamic force and moment. Graphs are generated showing the variation of the forces and moments with selected parameters, including the errors incurred by neglecting the random motion of the atmosphere.

15. SUBJECT TERMS

Spacecraft aerodynamics, Spacecraft atmospheric torques, Free molecular flow, Gas-surface intera

16. SECURITY CLASSIFICATION OF:			17. LIMITATION OF ABSTRACT	18. NUMBER OF PAGES	19a. NAME OF RESPONSIBLE PERSON
					Joel Storch
a. REPORT	b. ABSTRACT	c. THIS PAGE			19b. TELEPHONE NUMBER *(include area code)*
UNCLASSIFIED	UNCLASSIFIED	UNCLASSIFIED		63	(310)336-5932

Contents

List of Figures

1. Introduction

This report addresses the aerodynamic forces and moments on spacecraft due to their motion through a rarefied atmosphere. The impetus for this work arises from a desire to capitalize upon the features of an existing Aerospace developed tool, ATRIUM, which performs detailed thermal analyses of complex spacecraft configurations. The code utilizes randomly distributed ray tracings in conjunction with a suite of geometric primitives to calculate surface temperature gradients due to sun illumination and accounts for both multiple surface reflections and shadowing. In mathematical terms, ATRIUM provides a method to perform surface integrals of incident rays over complex geometries and thus can be exploited to calculate aerodynamic forces and torques for free-molecular flow.

On typical satellite configurations at altitudes below 370 km, the aerodynamic torque frequently dominates [1][†] and can have a value in the neighborhood of 0.0136 Nm. Although the magnitude of this torque is small by terrestrial standards (as are the other environmental disturbances), it has a nonnegligible affect on spacecraft motion over an extended period of time. Accurate predictions of the aerodynamic disturbances requires knowledge of the atmospheric density, surface relative molecular velocity and surface reflection properties. Even at fixed altitude there will be variations in the density due to Earth's diurnal cycle and solar activity. To correctly compute the surface relative molecular velocity, it is not sufficient to know the inertial motion of the spacecraft; the motion of the atmosphere is also required. Surface reflection properties are not well known for many materials and experimental data indicate that they vary with surface temperature and contamination as well as angle of attack of the incoming flow relative to the surface. In this study, we adopt a simple gas-surface interaction model parameterized by two empirical coefficients [2]. There is a substantial literature on this specific topic and a variety of models which have been tested against experimental data. It should be noted that most density models of the upper atmosphere were developed by observing the orbital decay of satellites and are based upon an *assumed value* of the drag coefficient. The drag coefficient however is critically dependent on the nature of the gas-surface interaction. It is seen therefore, that proper modeling of the gas-surface interaction is critical in obtaining accurate estimates of the aerodynamic disturbances.

At altitudes above 120-150 km, the atmospheric density is sufficiently low that conventional continuum assumptions are no longer valid. A dimensionless parameter, the *Knudsen number*, is used to classify the flow regime along the spectrum from continuum to highly rarefied. The Knudsen number, *Kn*, is defined by $Kn=\lambda/L$ where λ is the average mean free path of the molecules (the average distance traveled by a molecule before collision with another molecule) and L is a characteristic length representative of the spacecraft. By convention, a flow with $Kn < 0.01$ is regarded to be in the continuum regime where intermolecular collisions dominate. Flows with $Kn > 10$ are termed *free-molecular* where molecule-surface interactions govern the flow. Intermediate values of *Kn* correspond to the transition regime where molecule-molecule and molecule-surface interactions are of equal importance. Even for extremely low earth orbits, λ is almost 1 km. and hence the calculation of aerodynamic forces and torques upon the spacecraft must be based on free-molecular flow theory. It is the transfer of momentum to the surface by atmospheric molecules which determines the net force and torque. Momentum transfer occurs both when molecules arrive at the surface and upon subsequent reflection. The free-molecular assumption allows us to treat these cases

[†] numbers in brackets refer to the list of references

separately and add their effects. Momentum exchange due to molecules colliding with each other are neglected and only molecule-surface interactions are important. In addition, geometrically complicated surfaces can be easily treated by partitioning into simpler constituent surfaces except for complications due to shadowing and multiple surface collisions.

2. Nonrotating Bodies in Hyperthermal Free-molecular Flow

As mentioned in the Introduction, calculation of the aerodynamic force and moment on a spacecraft requires knowledge of the velocity of the impinging atmospheric molecules relative to the surface. In general, the spacecraft will be translating and rotating relative to the atmosphere and hence the surface relative velocity of the approaching molecules will vary over the surface. In addition, even for a purely translational motion, the molecules will have a distribution of velocities about a mean value dependent on the atmospheric temperature. In the present section we will assume that the spacecraft does not rotate relative to the atmosphere and we shall also neglect the random thermal motion of the atmospheric molecules. The later assumption is frequently refereed to as the *hyperthermal* approximation and is valid at sufficiently low temperatures when the random thermal motion of the molecules is negligible compared to the speed of the spacecraft. These simplifying assumptions allow us to treat the incoming molecules as a collimated beam impinging on an element of surface area with a single characteristic velocity (care being taken to only include those portions of the surface exposed to the oncoming flow). The effects of removing these assumptions will be addressed in subsequent sections.

2.1 Gas-Surface Interaction

In order to calculate the forces exerted upon the surface by the impinging molecules, we must specify the momentum exchange that occurs between the molecules and arresting surface. By convention, two canonical forms of surface reflection are defined. *Specular* reflection (Fig. 2.1) is a deterministic process in which the angle of incidence equals the angle of reflection while the incident velocity, reflected velocity and surface normal are all coplanar. The speeds of the incident and reflected molecules are not necessarily equal (some authors do however assume this equality in their definition). In the case of *diffuse* reflection (Fig. 2.2), the incident molecules are trapped into the interstices of the surface losing all knowledge of incoming direction and subsequently re-emitted from the surface with a random distribution of speed and random direction governed by a "cosine distribution" i.e. there are as many molecules with a particular speed leaving the surface in one direction as leaving in the opposite direction. For both modes of reflection, the speed with which the molecule leaves the surface is determined by the amount of energy it transfers to the surface before being re-emitted. The degree of equilibrium attained between the molecule and surface is measured by the energy accommodation coefficient σ_a defined by

$$\sigma_a = \frac{E_i - E_r}{E_i - E_w}$$

Where E_i ,E_r are the incident and reflected energy fluxes respectively and E_w is the energy flux that *would* be carried away by the reflected molecules if they were in thermal equilibrium with the surface. Thus σ_a=0 corresponds to no energy exchange between the incident molecules and the surface while σ_a=1 characterizes the incident molecules coming into equilibrium with the surface before being re-emitted.

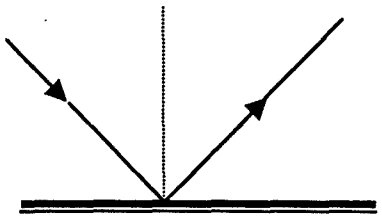

Figure 2.1. Specular Reflection.

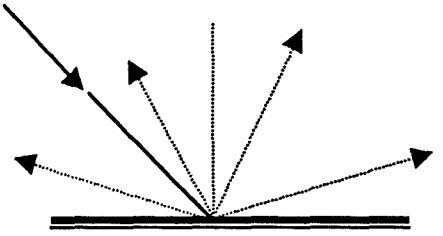

Figure 2.2. Diffuse Reflection.

We next introduce the momentum accommodation coefficients which relate the incident and reflected momentum fluxes. It is found [2] that better agreement is attained between theoretical calculations and experimental data if separate coefficients are assigned for normal and tangential momentum exchange. Resolving the molecular momentum into components normal and tangential to the surface, we define the respective momentum accommodation coefficients

$$\sigma_n \equiv \frac{p_i - p_r}{p_i - p_w}$$
$$\sigma_t \equiv \frac{\tau_i - \tau_r}{\tau_i - \tau_w} \qquad (2.1)$$

where p_i,p_r are the incident and reflected normal momentum flux and τ_i,τ_r are the incident and reflected tangential momentum flux. The parameters p_w,τ_w denote the normal and tangential components of momentum flux which *would* be carried away from the surface by the diffusely reflected molecules if they were in thermal equilibrium with the surface. Note that τ_w=0 by the definition of diffuse reflection. For completely diffuse reflection, σ_t=1 regardless of the degree of thermal accommodation while σ_n=1 additionally requires complete thermal accommodation. For complete specular reflection with no energy exchange between the molecules and the surface, σ_t=σ_n=0.

In order to calculate p_w, we must find an expression for the average normal velocity of diffusely reflected molecules which are in thermal equilibrium with the surface. With reference to Fig. 2.2, the molecules have become fully accommodated to the surface and leave with a random speed v characteristic of the surface temperature and at random direction θ (with respect to the surface normal) governed by a cosine distribution. The kinetic theory of gases (see Appendix A) provides us with the celebrated Maxwell-Boltzmann speed distribution for the molecules in equilibrium with the surface. If we denote this speed distribution by $\phi(v)$, then the probability that a molecule has speed in the range $(v, v+dv)$ and direction between θ and $\theta+d\theta$ is given by $\phi(v)\cos\theta\, dv\, d\theta$. The normal component of velocity is $v\cos\theta$, and hence the average normal velocity , V_w, is given by

$$V_w = \langle v\cos\theta \rangle = \int_0^{\pi/2}\int_0^{\infty} v\,\phi(v)\cos^2\theta\, dv d\theta$$

Performing the integration over θ and expressing the mean speed in terms of the surface temperature T_w [A.17, A.18] we obtain $V_w = (\pi k T_w/2m)^{1/2}$ where k is the Boltzmann constant (1.38065×10^{-23} joule/molecule° K) and m is the mass of a single gas molecule. Recalling that $k = \mathcal{R}/N_0$ where $\mathcal{R}$ is the universal gas constant (8314.5 joules/kg-mole°K) and N_0 is Avogadro's number (6.02214×10^{26} molecules/kg–mole), we can express V_w in the form

$$V_w = \sqrt{\frac{\pi \mathcal{R} T_w}{2\mathcal{M}}} \tag{2.2}$$

where $\mathcal{M}$ denotes the molecular weight. It sometimes proves convenient to express the above equation in terms of the gas constant R, which unlike $\mathcal{R}$, depends upon the particular gas of interest. In terms of the universal gas constant, the equation of state of an ideal gas is $pV = N\mathcal{R}T/N_0$ where p is the pressure, V is the volume, and N denotes the total number of molecules. Comparing this with the alternative form $p = \rho RT$ where ρ is the gas density, we find that $\mathcal{R}$=R$\mathcal{M}$. Hence eq.(2.2) can be expressed in the alternate form

$$V_w = \sqrt{\pi R T_w/2} \tag{2.3}$$

2.2 Aerodynamic Forces and Moments

Our first model is developed under the assumptions that 1) the body is not spinning relative to the atmosphere and 2) the mean thermal motion of the atmosphere is negligible compared to the speed of the body through the atmosphere; the so called *hyperthermal flow* assumption.

Figure 2.3 shows atmospheric molecules impinging upon the spacecraft surface S which is assumed to be convex so as to avoid complications due to shadowing. The molecules all have velocity $\vec{\mathbf{v}}$ relative to the surface so that the incident flow on an element of surface area dA can be viewed as a collimated molecular beam of mass density ρ. Denote by $\vec{\mathbf{n}}_{in}$ a unit *inward* drawn normal to the surface and let α be the angle between $\vec{\mathbf{n}}_{in}$ and $\vec{\mathbf{V}}$.

$$\cos\alpha = \hat{\mathbf{v}} \cdot \vec{\mathbf{n}}_{in} \tag{2.4}$$

Where $\hat{\mathbf{v}} = \vec{\mathbf{V}}/\|\vec{\mathbf{V}}\|$. It is important to note that no impingement occurs on those portions of the surface where $\cos\alpha < 0$. Hence we will insert the factor $H(\cos\alpha)$ (H denotes the Heaviside step function) into the surface integrals below to effectively limit the aerodynamic pressure to those portions of the surface which actually experience impingement. For an arbitrary surface S as shown in Fig. 2.3, there is no natural set of basis vectors to resolve the shear stress on the element of area dA so we will establish these vectors with respect to the direction $\hat{\mathbf{v}}$ of the incident molecules.

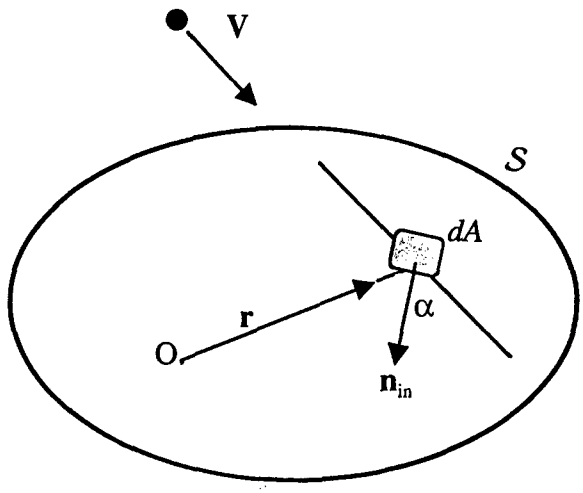

Figure 2.3. Spacecraft Surface in Free-Molecular Flow.

Decomposing $\hat{\mathbf{v}}$ into a component normal to the surface and its orthogonal projection into the tangent plane, we can write

$$\hat{\mathbf{v}} = \cos\alpha\,\vec{\mathbf{n}}_{in} + \sin\alpha\,\vec{\mathbf{t}} \qquad (2.5)$$

Which serves to define the unit tangent direction $\vec{\mathbf{t}}$. Forming the triple cross product $\vec{\mathbf{n}}_{in}\times\left(\hat{\mathbf{v}}\times\vec{\mathbf{n}}_{in}\right)$, yields the following expression for $\vec{\mathbf{t}}$ directly in terms of the unit vectors $\hat{\mathbf{v}}$ and $\mathbf{n}_{in}$

$$\vec{\mathbf{t}} = \frac{\vec{\mathbf{n}}_{in}\times\left(\hat{\mathbf{v}}\times\hat{\mathbf{n}}_{in}\right)}{\left\|\vec{\mathbf{n}}_{in}\times\left(\hat{\mathbf{v}}\times\hat{\mathbf{n}}_{in}\right)\right\|}$$

The vectors $\left\{\vec{\mathbf{t}}, \vec{\mathbf{n}}_{in}, \vec{\mathbf{t}}\times\vec{\mathbf{n}}_{in}\right\}$ constitute an orthonormal triad on the surface.

In a time interval Δt the mass delivered to dA is contained in a parallelepiped of base area dA and slant height $V\Delta t$ which constitutes a volume $V\Delta t\cos\alpha\,dA$. Thus the mass flux δQ is given by

$$\delta Q = \rho V\cos\alpha \qquad (2.6)$$

With the aid of eq.(2.5), the incident momentum flux $\vec{\mathbf{V}}\,\delta Q$ resolves into the components

$$\begin{aligned} p_i &= V\cos\alpha\,\delta Q \\ \tau_i &= V\sin\alpha\,\delta Q \end{aligned} \qquad (2.7)$$

Under steady state conditions the incident and reflected mass fluxes are equal; hence $p_w = V_w\,\delta Q$

where V_w is given by eq.(2.3). The reflected momentum flux is given by the expression: $-p_r\vec{\mathbf{n}}_{in}+\tau_r\vec{\mathbf{t}}$. Subtracting the reflected from the incident momentum flux yields the force per unit area, $d\vec{\mathbf{f}}/dA$, exerted by the molecules upon the surface.

$$\frac{d\vec{\mathbf{f}}}{dA}=(p_i+p_r)\vec{\mathbf{n}}_{in}+(\tau_i-\tau_r)\vec{\mathbf{t}} \tag{2.8}$$

The two components of reflected momentum flux can be expressed in terms of the incident fluxes, p_w, and momentum accommodation coefficients through eq.(2.1) By utilizing eqs.(2.6) & (2.7), we can write eq.(2.8) in the form

$$\frac{d\vec{\mathbf{f}}}{dA}=\rho V^2\cos\alpha\left\{\left[(2-\sigma_n-\sigma_t)\cos\alpha+\sigma_n\frac{V_w}{V}\right]\vec{\mathbf{n}}_{in}+\sigma_t\hat{\mathbf{v}}\right\} \tag{2.9}$$

where we have eliminated $\vec{\mathbf{t}}$ in terms of $\vec{\mathbf{n}}_{in}$ and $\hat{\mathbf{v}}$ through eq.(2.5). This form is simpler to integrate since $\hat{\mathbf{v}}$ (unlike $\vec{\mathbf{t}}$) will not vary over the surface. Integrating over those portions of the surface which are impinged by the atmospheric molecules, and assuming that the atmospheric density, accommodation coefficients, and surface temperature are constant over the surface, we obtain the net force **f** and moment **g** about point O (see Fig.2.3). All vectors are assumed to be resolved in a set of body–fixed axes and indicated by bold face type.

$$\mathbf{f}=\rho V^2\left[\sigma_t A_p\hat{\mathbf{v}}+\sigma_n(V_w/V)\mathcal{F}_1+(2-\sigma_n-\sigma_t)\mathcal{F}_2\right] \tag{2.10}$$

$$\mathbf{g}=\rho V^2\left[\sigma_t A_p\mathbf{c}_p\times\hat{\mathbf{v}}+\sigma_n(V_w/V)\mathcal{G}_1+(2-\sigma_n-\sigma_t)\mathcal{G}_2\right] \tag{2.11}$$

where the newly introduced terms are only dependent upon the surface geometry and angle between the incident flow and surface normal.

$$\begin{aligned}
A_p&=\iint H(\cos\alpha)\cos\alpha\,dA & A_p\mathbf{c}_p&=\iint H(\cos\alpha)\cos\alpha\,\mathbf{r}\,dA\\
\mathcal{F}_1&=\iint H(\cos\alpha)\cos\alpha\,\mathbf{n}_{in}\,dA & \mathcal{F}_2&=\iint H(\cos\alpha)\cos^2\alpha\,\mathbf{n}_{in}\,dA\\
\mathcal{G}_1&=\iint H(\cos\alpha)\cos\alpha\,\mathbf{r}\times\mathbf{n}_{in}\,dA & \mathcal{G}_2&=\iint H(\cos\alpha)\cos^2\alpha\,\mathbf{r}\times\mathbf{n}_{in}\,dA
\end{aligned} \tag{2.12}$$

2.3 Closed Form Solutions

As a means of checking the implementation of the aerodynamic force and torque calculation, we provide closed-form solutions for the following geometric shapes.

- Sphere
- Flat Plate
- Right Circular Cylinder
- Circular Cone Frustum

The force and moment components are plotted as functions of the angle of attack (except for the sphere)

2.3.1 Sphere in Hyperthermal Free-molecular Flow

Figure 2.4 shows a sphere of radius a with a system of spherical coordinates $\{r,\theta,\varphi\}$ at its center. Without loss of generality, we may assume that the incident molecular flow **V** is directed along the z axis. The surface of the sphere is described by: $r=a$, $0\le\theta\le\pi$, $0\le\varphi\le 2\pi$ with element of surface area $dA = a^2 \sin\theta\, d\theta\, d\varphi$. The unit inward normal is given by

$$\mathbf{n}_{in} = -\sin\theta\cos\varphi\,\mathbf{i} - \sin\theta\sin\varphi\,\mathbf{j} - \cos\theta\,\mathbf{k}$$

where **i**,**j**,**k** denote unit vectors along the axes of x,y,z respectively. Recognizing that the factor $H(\cos\alpha)$ limits the integration to $\pi/2\le\theta\le\pi$, the surface integrals are readily computed and have the values: $A_p=\pi a^2$, $\mathcal{F}_1=2\pi a^2/3\ \mathbf{k}$, $\mathcal{F}_2=\pi a^2/2\ \mathbf{k}$. Hence the net force on the sphere is a drag with magnitude D given by

$$D=\frac{1}{2}\pi a^2\rho V^2\left(2+\sigma_t-\sigma_n+\frac{4}{3}\sigma_n\frac{V_w}{V}\right) \tag{2.13}$$

It is clear from symmetry (and verified by calculation) that the aerodynamic torque about the center of the sphere is zero.

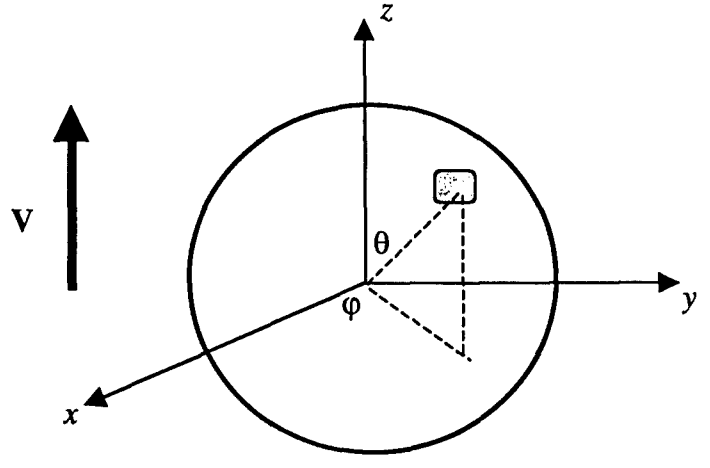

Figure 2.4. Sphere in Free-Molecular Flow.

2.3.2 Flat Plate in Hyperthermal Free-molecular Flow

Figure 2.5 shows a flat plate of area A at angle of attack β with respect to the incident molecular velocity **V**. A rectangular coordinate system is established with origin at the centroid of the plate with x,y axes respectively parallel and perpendicular to **V**. Here $\cos\alpha = \sin\beta \geq 0$ for angles of attack between zero and 180 degrees. Since the surface is flat, the integrals are trivial to evaluate.

$$A_p = A\sin\beta, \quad \mathcal{F}_1 = A\sin\beta\,\mathbf{n}_{\text{in}}, \quad \mathcal{F}_2 = A\sin^2\beta\,\mathbf{n}_{\text{in}}$$

The resolution of the inner surface normal (with respect to the direction of incident flow) along the drag (x) and lift (y) directions is given by $\mathbf{n}_{\text{in}} = \sin\beta\,\mathbf{i} + \cos\beta\,\mathbf{j}$. The net force on the plate then assumes the form

$$\mathbf{f} = \frac{1}{2}\rho V^2 A\left(C_D\,\mathbf{i} + C_L\,\mathbf{j}\right)$$

Where the lift and drag coefficients are given by

$$C_L = \left[\sigma_n \frac{V_w}{V} + \left(2 - \sigma_n - \sigma_t\right)\sin\beta\right]\sin 2\beta \tag{2.14}$$

$$C_D = 2\left[\sigma_t + \sigma_n \frac{V_w}{V}\sin\beta + \left(2 - \sigma_n - \sigma_t\right)\sin^2\beta\right]\sin\beta \tag{2.15}$$

It is readily shown that the aerodynamic moment about the centroid of the plate is zero.

The lift and drag coefficients are plotted below as functions of the angle of attack for $\sigma_n = \sigma_t = 0.7$ and $V_w/V = 0.05$. In general, the drag attains its maximum value at $\beta = \pi/2$ being symmetric about this point and vanishing when $\beta = 0, \pi$ while the lift is antisymmetrical about $\beta = \pi/2$ vanishing at the points $\beta = 0, \pi/2, \pi$.

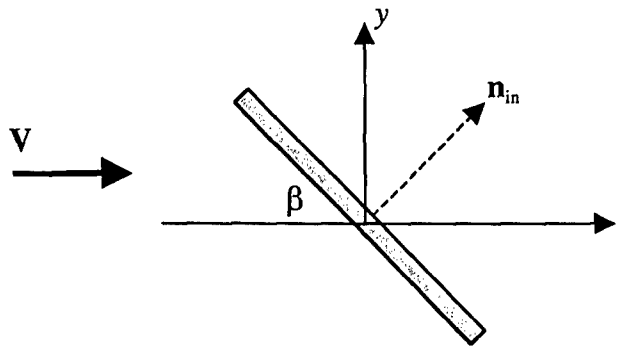

Figure 2.5. Flat Plate in Free-Molecular Flow.

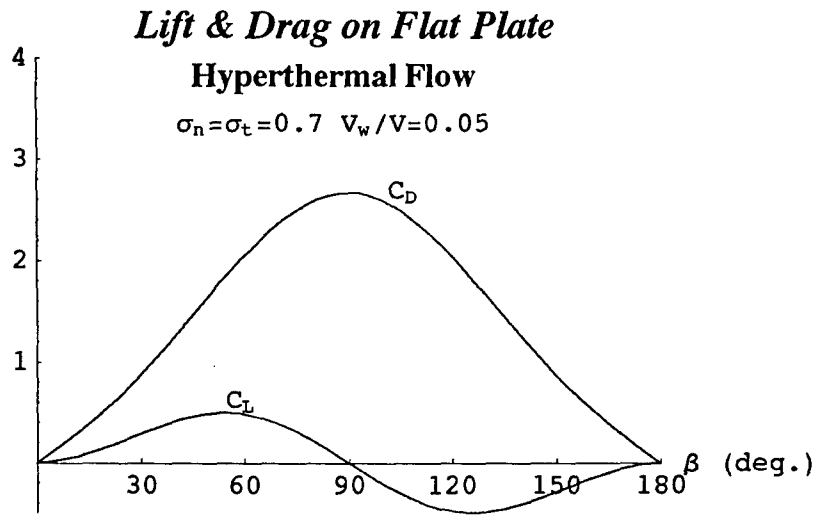

Figure 2.6. C_L & C_D for Flat Plate in Hyperthermal Free-Molecular Flow.

2.3.3 Right Circular Cylinder in Hyperthermal Free-molecular Flow

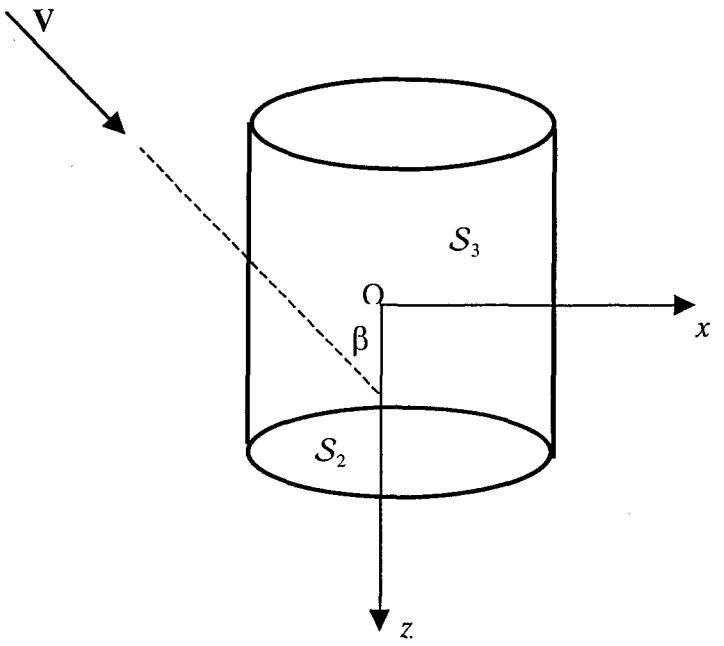

Figure 2.7. Cylinder in Free-molecular Flow

Figure 2.7 shows a right circular cylinder of length l and base radius a at angle of attack β with respect to the incident molecular velocity **V**. A rectangular coordinate system with origin at the centroid O of the cylinder has its z axis along the axis of the cylinder and x axis in the plane determined by **V** and the cylinder axis. It suffices to consider angles of attack in the range $0 \le \beta \le \pi/2$. For purposes of computing the surface integrals, we partition the cylindrical surface into its end bases S_1,S_2 and lateral surface S_3.

• Force & Moment on Lateral Surface

In terms of the cylindrical coordinates $(r,\theta,z)(x = r\cos\theta, y = r\sin\theta)$, the surface S_3 is described by $r = a, 0 \le \theta \le 2\pi, -l/2 \le z \le l/2$ and the element of surface area is given by $dA = a\,d\theta\,dz$. Observing that $\mathbf{n}_{in} = -\cos\theta\,\mathbf{i} - \sin\theta\,\mathbf{j}$ and $\hat{\mathbf{v}} = \sin\beta\,\mathbf{i} + \cos\beta\,\mathbf{k}$, we have $\cos\alpha = -\sin\beta\cos\theta$; thus the region of integration will be limited to $\pi/2 \le \theta \le 3\pi/2$ for the specified range of angle of attack. Straightforward integration yields the following expressions over the lateral surface.

$$A_p = 2al\sin\beta \qquad A_p\mathbf{c}_p = -\pi/2\,a^2 l\sin\beta\,\mathbf{i} \qquad \mathcal{G}_1 = \mathbf{0}$$
$$\mathcal{F}_1 = \pi/2\,al\sin\beta\,\mathbf{i} \qquad \mathcal{F}_2 = 4/3\,al\sin^2\beta\,\mathbf{i} \qquad \mathcal{G}_2 = \mathbf{0}$$

Resolving the force and moment along the $\{x,y,z\}$ axes, we find the force $\mathbf{f}_3$ and moment $\mathbf{g}_3$ (about point O) on the lateral surface.

$$\mathbf{f}_3 = \rho V^2 al\left\{\left[\frac{\pi}{2}\sigma_n\frac{V_w}{V}+\left(\frac{8}{3}-\frac{4}{3}\sigma_n+\frac{2}{3}\sigma_t\right)\sin\beta\right]\sin\beta\,\mathbf{i}+\sigma_t\sin 2\beta\,\mathbf{k}\right\} \tag{2.16}$$

$$\mathbf{g}_3 = \pi/4\,\rho V^2 a^2 l\sigma_t \sin 2\beta\,\mathbf{j} \tag{2.17}$$

• Force & Moment on End Surfaces

The end face S_2 of the cylinder is not impinged upon by the flow over the specified range of angle of attack. To calculate the force and torque on S_1, we apply the results obtained above for the flat plate with $A=\pi a^2$ (see eqs.(2.14) & (2.15)) Noting from Fig.2.7 that the angle of attack of S_1 with respect to $\mathbf{V}$ is $\beta+\pi/2$, and resolving the drag and lift forces along the coordinate directions $\{x,y.z\}$, we find that the force $\mathbf{f}_1$ on S_1 is given by

$$\mathbf{f}_1 = \pi/2\,a^2\rho V^2\left\{\sigma_t\sin 2\beta\,\mathbf{i}+2\cos\beta\left[\sigma_n\frac{V_w}{V}+(2-\sigma_n)\cos\beta\right]\mathbf{k}\right\} \tag{2.18}$$

The aerodynamic moment on S_1 about point O is: $-l/2\,\mathbf{k}\times\mathbf{f}_1$ which can be shown to be equal to $-\mathbf{g}_3$.

• Net Force & Moment on Cylinder

Adding the contributions from S_1 and S_3 we find that the net force f on the cylinder can be written in the form $f=f_x\,\mathbf{i}+f_z\,\mathbf{k}$ where

$$\begin{aligned} f_x &= \frac{1}{6}al\rho V^2\sin\beta\left[4(4+\sigma_t-2\sigma_n)\sin\beta+6\pi\frac{a}{l}\sigma_t\cos\beta+3\pi\sigma_n\frac{V_w}{V}\right] \\ f_z &= al\rho V^2\cos\beta\left[2\sigma_t\sin\beta+\pi\frac{a}{l}(2-\sigma_n)\cos\beta+\pi\frac{a}{l}\frac{V_w}{V}\sigma_n\right] \end{aligned} \tag{2.19}$$

The net moment about the centroid of the cylinder is zero at any angle of attack.

The two force components are plotted below as functions of the angle of attack for $\sigma_n=\sigma_t=0.7$ $V_w/V=0.05$, and $a/l=0.2$.

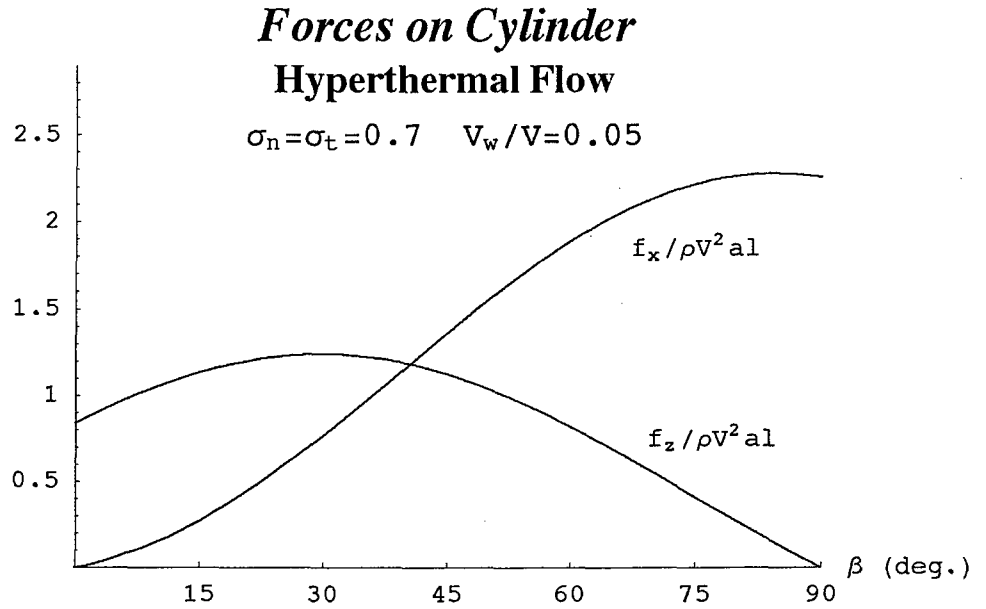

Figure 2.8. Forces on Cylinder in Hyperthermal Free-molecular Flow.

2.3.4 Cone Frustum in Hyperthermal Free-molecular Flow

Figure 2.9 shows a cone frustum of circular cross section in a free-molecular flow where the incident velocity **V** is at an angle of attack β with respect to its axis of symmetry. The end surfaces S_1,S_2 of the body are circular disks of radii R_1,R_2 respectively and γ denotes the half angle of the cone. We restrict our attention to the range of angles $0<\gamma<\pi/2$, $0\le\beta<\pi/2$. A rectangular coordinate system $\{x,y,z\}$ is introduced with origin at the apex of the cone and z axis coincident with the axis of symmetry. Without loss of generality, we choose the x axis such that **V** lies in the x-z plane. In terms of cylindrical coordinates $\{r,\theta,z\}$, the lateral surface S_3 of the cone frustum is described by: $0\le\theta\le 2\pi$, $z_1\le z\le z_2$ where $z_i = R_i\cot\gamma\ (i=1,2)$ and $r(z)=\tan\gamma\, z$. On S_3, the position vector to an arbitrary point is given by $\mathbf{r}=\tan\gamma\, z\cos\theta\,\mathbf{i}+\tan\gamma\, z\sin\theta\,\mathbf{j}+z\mathbf{k}$ and the element of surface area is $dA=\sin\gamma/\cos^2\gamma\ z\,dz\,d\theta$. From the figure, $\mathbf{n}_{in}=-\cos\gamma\cos\theta\,\mathbf{i}-\cos\gamma\sin\theta\,\mathbf{j}+\sin\gamma\,\mathbf{k}$ on S_3 and $\hat{\mathbf{v}}=\sin\beta\,\mathbf{i}+\cos\beta\,\mathbf{k}$. Forming the inner product of these two vectors we find

$$\cos\alpha=\cos\beta\sin\gamma-\sin\beta\cos\gamma\cos\theta \qquad (2.20)$$

To determine the portions of S_3 that are impinged by the atmospheric molecules, we need to determine the sign of $\cos\alpha$ for $0\le\theta\le 2\pi$. Since $\cos\alpha$ vanishes when $\cos\theta=\tan\gamma/\tan\beta$, we consider separately the two cases: 1) $0\le\beta<\gamma$ and 2) $\gamma<\beta<\pi/2$.

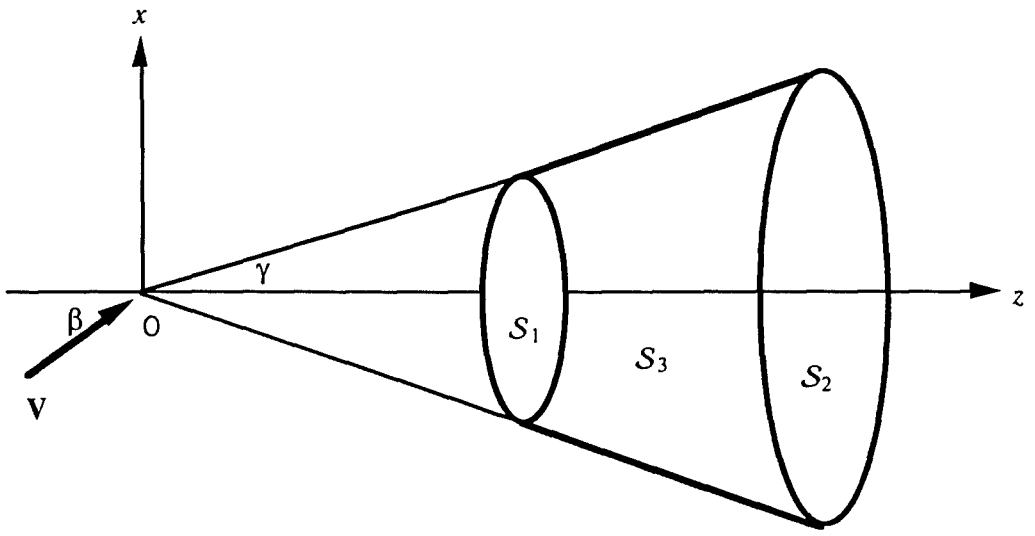

Figure 2.9. Cone frustum in Free-molecular Flow.

• Case 1: $0 \le \beta < \gamma$

It is clear from eq.(2.20) that in this case $\cos\alpha > 0$ for all values of θ, hence the entire lateral surface of the cone intercepts the molecular flux. Performing the integrations indicated in eq.(2.12) we obtain

$$
\begin{aligned}
A_p &= \pi\left(R_2^2 - R_1^2\right)\cos\beta \\
\mathcal{F}_1 &= \frac{\pi}{2}\left(R_2^2 - R_1^2\right)\left(\cot\gamma\cos\gamma\sin\beta\,\mathbf{i} + 2\sin\gamma\cos\beta\,\mathbf{k}\right) \\
\mathcal{F}_2 &= \frac{\pi}{2}\left(R_2^2 - R_1^2\right)\left[\cos^2\gamma\,\sin 2\beta\,\mathbf{i} + \frac{1}{4}\left(3 + \cos 2\beta - \cos 2\gamma - 3\cos 2\beta\cos 2\gamma\right)\mathbf{k}\right] \\
A_p\mathbf{c}_p &= \frac{\pi}{3}\cot\gamma\left(R_2^3 - R_1^3\right)\left(-\sin\beta\,\mathbf{i} + 2\cos\beta\,\mathbf{k}\right) \\
\mathcal{G}_1 &= \frac{\pi}{3}\left(R_2^3 - R_1^3\right)\sin\beta\cot\gamma\csc\gamma\,\mathbf{j} \\
\mathcal{G}_2 &= \frac{\pi}{3}\left(R_2^3 - R_1^3\right)\sin 2\beta\cot\gamma\,\mathbf{j}
\end{aligned}
$$

The force $\mathbf{f}_3$ and moment $\mathbf{g}_3$ (about point O) on the lateral surface follow from eqs. (2.10) & (2.11).

$$
\begin{aligned}
\mathbf{f}_3 = \tilde{f}\Big[&\sigma_t\sin 2\beta + \sigma_n\frac{V_n}{V}\cot\gamma\cos\gamma\sin\beta + \left(2 - \sigma_n - \sigma_t\right)\cos^2\gamma\,\sin 2\beta\Big]\mathbf{i} + \\
&\tilde{f}\Big[2\sigma_t\cos^2\beta + 2\sigma_n\frac{V_n}{V}\sin\gamma\cos\beta + \\
&\frac{1}{4}\left(2 - \sigma_n - \sigma_t\right)\left(3 + \cos 2\beta - \cos 2\gamma - 3\cos 2\gamma\cos 2\beta\right)\Big]\mathbf{k}
\end{aligned}
\qquad (2.21)
$$

$$\mathbf{g}_3 = \frac{\pi}{3}\rho V^2\left(R_2^3 - R_1^3\right)\left[\sigma_n \frac{V_w}{V}\csc\gamma + \left(4 - 2\sigma_n + \sigma_t\right)\cos\beta\right]\cot\gamma\sin\beta\,\mathbf{j} \qquad (2.22)$$

where $\tilde{f} = \frac{1}{2}\rho V^2\pi\left(R_2^2 - R_1^2\right)$

We note that in the limit as $\gamma \to \pi/2$, the lateral surface degenerates into an annular disk and the above expressions are in agreement with those obtained previously for a flat plate (see eqs.(2.14),(2.15)) corresponding to the area $A = \pi\left(R_2^2 - R_1^2\right)$.

• Case 2: $\gamma < \beta \le \pi/2$

To establish the θ limits of integration in this case, we have plotted in Figure 2.10 the function $\cos\alpha$ of eq.(2.20) for θ over the interval $(0,2\pi)$. We note that this function is negative at θ=0, positive at θ=π, and symmetric about the latter point. The root θ^* of the function in the interval $(0,\pi)$ is given by

$$\theta^* = \cos^{-1}\left(\tan\gamma/\tan\beta\right) \qquad (2.23)$$

hence the integration limits in this case are $\theta^* \le \theta \le 2\pi - \theta^*;\ z_1 \le z \le z_2$.

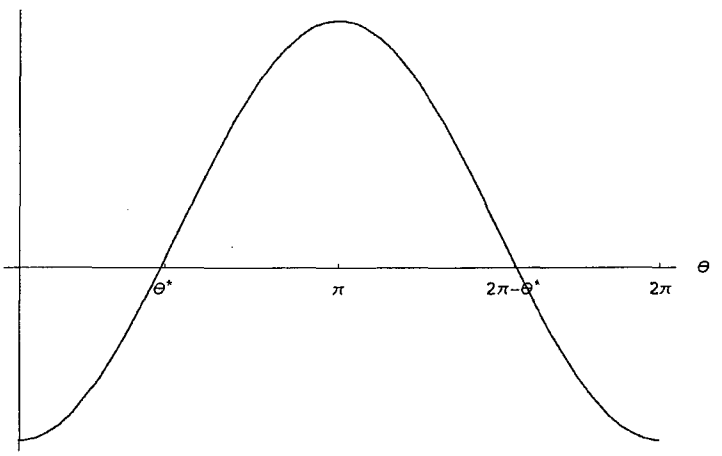

Figure 2.10. Plot of $\cos\alpha(\theta)$ for $\beta > \gamma$.

We will have a continuous transition from Case 1 since $\theta^* \to 0$ as $\beta \to \gamma^+$. Performing the integrations indicated in eq.(2.12) we obtain

$$A_p = \left(R_2^2 - R_1^2\right)\left[\left(\pi - \theta^*\right)\cos\beta + \cot\gamma\sin\theta^*\sin\beta\right]$$

$$\mathcal{F}_1 = \frac{1}{2}\left(R_2^2 - R_1^2\right)\cos\gamma\left[\left(\pi - \theta^* - \sin\theta^*\cos\theta^*\right)\cot\gamma\sin\beta + 2\sin\theta^*\cos\beta\right]\mathbf{i} +$$
$$\left(R_2^2 - R_1^2\right)\left[\left(\pi - \theta^*\right)\sin\gamma\cos\beta + \cos\gamma\sin\theta^*\sin\beta\right]\mathbf{k}$$

$$\mathcal{F}_2 = \frac{1}{8}\left(R_2^2 - R_1^2\right)\cos\gamma\left[2\cos\gamma\left(2\pi - 2\theta^* - \sin 2\theta^*\right)\sin 2\beta + 8\sin\gamma\sin\theta^*\cos^2\beta +\right.$$
$$\frac{2}{3}\cos\gamma\cot\gamma\left(9\sin\theta^* + \sin 3\theta^*\right)\sin^2\beta\left.\right]\mathbf{i} +$$
$$\frac{1}{4}\left(R_2^2 - R_1^2\right)\cos^2\gamma\left[4\left(\pi - \theta^*\right)\sec^2\gamma\cos^2\beta + \theta^* + 3\left(\theta^* - \pi\right)\cos 2\beta +\right.$$
$$\left.4\tan\gamma\sin\theta^*\sin 2\beta - \sin 2\theta^*\sin^2\beta - \pi\right]\mathbf{k}$$

$$A_p\mathbf{c}_p = -\frac{1}{3}\left(R_2^3 - R_1^3\right)\left[2\sin\theta^*\cos\beta + \cot\gamma\left(\pi - \theta^* - \sin\theta^*\cos\theta^*\right)\sin\beta\right]\mathbf{i} +$$
$$\frac{2}{3}\left(R_2^3 - R_1^3\right)\cot\gamma\left[\left(\pi - \theta^*\right)\cos\beta + \cot\gamma\sin\theta^*\sin\beta\right]\mathbf{k}$$

$$\mathcal{G}_1 = \frac{1}{3}\left(R_2^3 - R_1^3\right)\cot\gamma\csc\gamma\left[\left(\pi - \theta^* - \sin\theta^*\cos\theta^*\right)\sin\beta + 2\tan\gamma\sin\theta^*\cos\beta\right]\mathbf{j}$$

$$\mathcal{G}_2 = \frac{1}{12}\left(R_2^3 - R_1^3\right)\left[8\sin\theta^*\cos^2\beta - 2\cot\gamma\left(2\theta^* + \sin 2\theta^* - 2\pi\right)\sin 2\beta +\right.$$
$$\left.\frac{2}{3}\cot^2\gamma\left(9\sin\theta^* + \sin 3\theta^*\right)\sin^2\beta\right]\mathbf{j}$$

The force and moment (about point O) exerted upon the surface S_3 can now be calculated from eqs.(2.10) & (2.11). As in case 1, the force lies in the x-z plane and the moment is directed along the y axis.

Combining the results from the above two cases allows us to compute the aerodynamic force and moment on the *lateral surface* of the cone frustum over the full range of angle of attack $\left(0 \le \beta \le \pi/2\right)$ as illustrated in the two plots below. The numerical results were generated for a cone half-angle of 60 deg., σ_n=σ_t=0.7, and V_w/V=0.05. The force and moment were rendered dimensionless by dividing by the respective scale factors $1/2\,\rho V^2\pi\left(R_2^2 - R_1^2\right)$ and $1/3\,\rho V^2\pi\left(R_2^3 - R_1^3\right)$. To find the *net* force and moment on the cone frustum, we simply add the contribution from the end surface S_1 which is a flat plate of area πR_1^2 (see eqs. (2.14) & (2.15)).

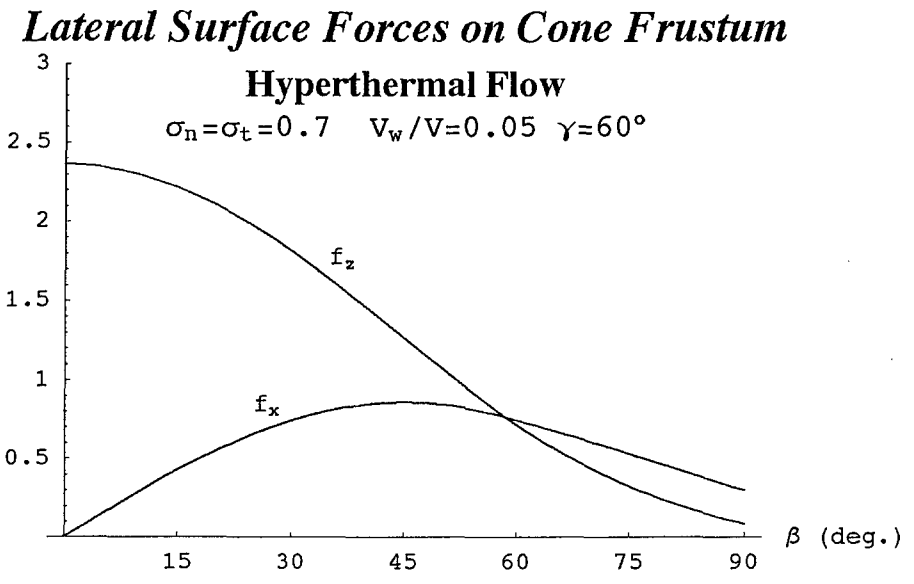

Figure 2.11. Forces on Cone Frustum in Hyperthermal Free-molecular Flow.

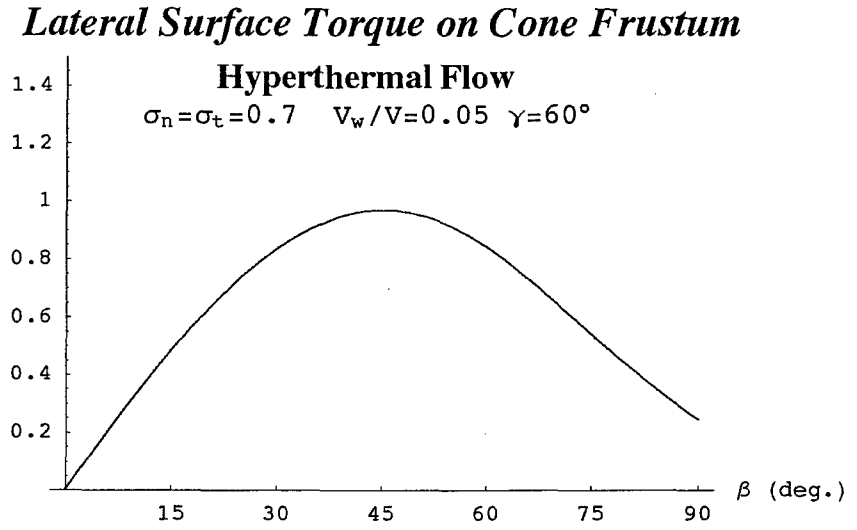

Figure 2.12. Torque on Cone Frustum in Hyperthermal Free-molecular Flow.

3. Nonrotating Bodies in Free-molecular Flow

In the previous section, the model for predicting the aerodynamic disturbances on a body in a free-molecular flow was based upon the assumption that the body was undergoing a pure translation relative to the atmosphere and that the random thermal motion of the atmospheric gas molecules was negligible in comparison with the speed of the body relative to the atmosphere. In this section we develop expressions for the aerodynamic force and torque which include the effects of the random thermal motion of the gas molecules (the body is still assumed not to rotate relative to the mean motion of the atmosphere). As will be seen, the quadratures which are called for in calculating the net force an torque are much more complicated that those derived previously under the hyperthermal flow assumption.

3.1 Aerodynamics of a Body Translating in a Maxwellian Flow

If we consider a gas in equilibrium, then the number of molecules with random velocities between **u** and **u+du** is given by [A.19]

$$\frac{N}{\pi^{3/2}}\left(\frac{mN_0}{2\mathcal{R}T_a}\right)^{3/2}\exp\left(-\frac{mN_0}{2\mathcal{R}T_a}u^2\right)du_1\,du_2\,du_3$$

where N is the total number of molecules, m is the mass of a single gas molecule and T_a is the atmospheric temperature. The constants $\mathcal{R}$ and N_0 denote the universal gas constant and Avagadro's number respectively. Dividing this expression by the gas volume and recognizing the product mN_0 as the gas molecular weight $\mathcal{M}$, we find that the number of molecules per unit volume with random velocities between **u** and **u+du** can be expressed in the form

$$\frac{\rho}{mV_a^3\pi^{3/2}}\exp\left(-\frac{u^2}{V_a^2}\right)du_1\,du_2\,du_3 \tag{3.1}$$

where ρ is the gas density and the parameter V_a represents the most probable speed [A.16].

$$V_a=\sqrt{\frac{2\mathcal{R}T_a}{\mathcal{M}}} \tag{3.2}$$

The random velocity **u** appearing above is with respect to the mean motion of the gas. Denoting by **V** the mean velocity of the gas, and resolving along the unit triad $\{\mathbf{n}_{in},\mathbf{t},\mathbf{n}_{in}\times\mathbf{t}\}$ at the element of surface area dA (see Fig. 3.1), we can write

$$\mathbf{V}=\mathrm{V}\left(\cos\alpha\,\mathbf{n}_{in}+\sin\alpha\,\mathbf{t}\right).$$

It follows that the velocity **v** of the molecules with respect to the surface is given by $\mathbf{v}=\mathbf{V}+\mathbf{u}$. Writing $\mathbf{v}=\mathrm{v}_1\mathbf{n}_{in}+\mathrm{v}_2\mathbf{t}+\mathrm{v}_3\,\mathbf{n}_{in}\times\mathbf{t}$, we can express the square of the random speed in the form

$$u^2=(\mathbf{v}-\mathbf{V})\cdot(\mathbf{v}-\mathbf{V})=\mathrm{v}^2+\mathrm{V}^2-2\mathrm{V}\left(\mathrm{v}_1\cos\alpha+\mathrm{v}_2\sin\alpha\right)$$

Hence the number of molecules per unit volume whose surface relative velocity lie between **v** and **v+dv** is given by $f(\mathrm{v}_1,\mathrm{v}_2,\mathrm{v}_3)\,d\mathrm{v}_1d\mathrm{v}_2\,d\mathrm{v}_3$ where

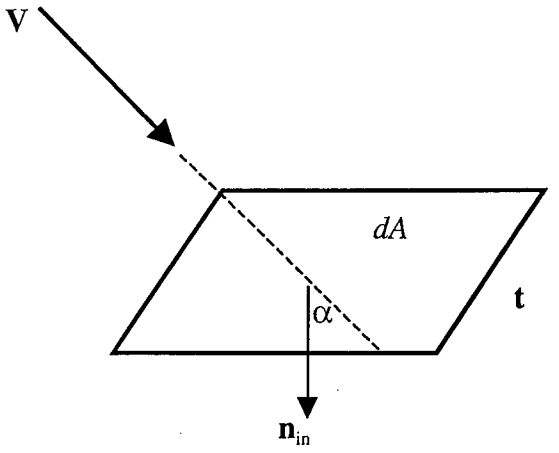

Figure 3.1. Unit Triad on Surface

$$f(\mathrm{v}_1,\mathrm{v}_2\mathrm{v}_3)=\frac{\rho\exp(-S^2)}{mV_a^3\pi^{3/2}}\exp\left(-\frac{\mathrm{v}^2}{V_a^2}\right)\exp\left[\frac{2S}{V_a}(\mathrm{v}_1\cos\alpha+\mathrm{v}_2\sin\alpha)\right] \tag{3.3}$$

and S denotes the molecular speed ratio

$$S=\frac{V}{V_a} \tag{3.4}$$

Our first model, based upon the hyperthermal flow assumption, corresponds to $S=\infty$ (in the sense that V_a=0).

Consider a stream of molecules with velocities in the range (**v**,**v**+d**v**) incident upon the element of surface area dA. In a short time interval Δt, these molecules sweep out a volume $dA\,\mathrm{v}_1\Delta t$. Thus $f(\mathbf{v})d\mathrm{v}_1 d\mathrm{v}_2 d\mathrm{v}_3\,dA\,\mathrm{v}_1\Delta t\,m$ is the mass delivered to dA in time Δt from molecules with surface relative velocity in the range (**v**,**v**+d**v**). The net mass flux δQ from all incident molecules is given by

$$\delta Q=m\int_{-\infty}^{\infty}\int_{-\infty}^{\infty}\int_{0}^{\infty}f(\mathrm{v}_1,\mathrm{v}_2,\mathrm{v}_3)\mathrm{v}_1\,d\mathrm{v}_1 d\mathrm{v}_2 d\mathrm{v}_3$$

Note the integration limits on v_1; a molecule with $\mathrm{v}_1<0$ is traveling *away* from the surface. Utilizing eq.(3.3) and performing the integration, we obtain

$$\delta Q=\rho V_a\Gamma_1(S\cos\alpha) \tag{3.5}$$

where

$$\Gamma_1(x)=\frac{1}{2\sqrt{\pi}}\left[\exp(-x^2)+\sqrt{\pi}x(1+\mathrm{erf}\,x)\right] \tag{3.6}$$

The incident momentum flux due to molecules with surface relative velocities in the range (**v**,**v**+d**v**), is given by

$$mf(\mathbf{v})v_1\left(v_1\mathbf{n}_{in}+v_2\mathbf{t}+v_3\mathbf{n}_{in}\times\mathbf{t}\right)dv_1dv_2dv_3$$

Integrating over the region $\{0\le v_1<\infty,-\infty<v_2<\infty,-\infty<v_3<\infty\}$ and noting that $f(\mathbf{v})$ is an even function of v_3 (so that the last component integrates to zero) we arrive at the following expressions for the components of the incident momentum flux along the normal and tangential directions to the element of surface area.

$$\begin{aligned} p_i &= \rho V_a^2\,\Gamma_2(S\cos\alpha) \\ \tau_i &= \rho V_a^2 S\sin\alpha\,\Gamma_1(S\cos\alpha) \end{aligned} \tag{3.7}$$

where
$$\Gamma_2(x)=\frac{1}{2\sqrt{\pi}}\left[x\exp\left(-x^2\right)+\left(\sqrt{\pi}/2\right)\left(1+2x^2\right)\left(1+\operatorname{erf}x\right)\right] \tag{3.8}$$

The functions $\Gamma_1(x)$ and $\Gamma_2(x)$ are plotted below in Figure 3.2

Under steady state conditions, the incident and reflected mass fluxes are equal; hence $p_w=V_w\,\delta Q$ where V_w and δQ are given by eqs.(2.2) & (3.5) respectively. The force per unit area is given by eq.(2.8), where again, the two components of reflected momentum flux can be expressed in terms of the incident fluxes, p_w, and momentum accommodation coefficients through eq.(2.1). Utilizing eqs.(3.5) & (3.7) we finally arrive at the result

$$\begin{aligned} \frac{df}{dA} = \rho V_a^2\left[\left(2-\sigma_n\right)\Gamma_2(S\cos\alpha)-\sigma_t S\cos\alpha\,\Gamma_1(S\cos\alpha)+\sigma_n\frac{V_w}{V_a}\Gamma_1(S\cos\alpha)\right]\mathbf{n}_{in}+ \\ \rho V_a^2\sigma_t S\,\Gamma_1(S\cos\alpha)\hat{\mathbf{v}} \end{aligned} \tag{3.9}$$

where we have eliminated $\mathbf{t}$ in terms of $\mathbf{n}_{in}$ and $\hat{\mathbf{v}}$ through eq.(2.5) (recall that $\hat{\mathbf{v}}=\mathbf{V}/\|\mathbf{V}\|$)

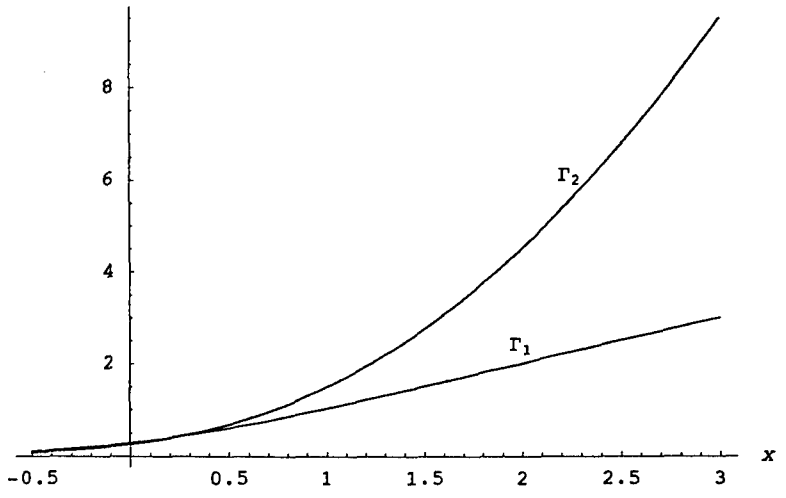

Figure 3.2. Universal Functions Γ_1 and Γ_2.

In contrast to the hyperthermal case treated earlier, *all* portions of the (convex) surface experience impingement due to the random motion of the molecules; hence we do not restrict the integration to those portions of the surface where $\cos\alpha \geq 0$. As would be expected, the molecular flux is maximum at α=0 and minimum at α=π (see eq.(3.5) and Fig. 3.2). Integrating eq.(3.9) over the entire surface and assuming that the atmospheric density, accommodation coefficients, and surface temperature are constant, we obtain the net force $\boldsymbol{f}$ in the form

$$\boldsymbol{f} = \rho V^2 \left[\frac{\sigma_t}{S} \mathrm{F}_1 \hat{\mathbf{v}} + \frac{2-\sigma_n}{S^2} \mathcal{F}_2 - \frac{\sigma_t}{S} \mathcal{F}_3 + \frac{\sigma_n}{S} \frac{V_w}{V} \mathcal{F}_4 \right] \tag{3.10}$$

where

$$\begin{aligned} \mathcal{F}_1 &= \iint \Gamma_1(S\cos\alpha)\, dA & \mathcal{F}_2 &= \iint \Gamma_2(S\cos\alpha)\, \mathbf{n}_{\text{in}}\, dA \\ \mathcal{F}_3 &= \iint \Gamma_1(S\cos\alpha)\cos\alpha\, \mathbf{n}_{\text{in}}\, dA & \mathcal{F}_4 &= \iint \Gamma_1(S\cos\alpha)\, \mathbf{n}_{\text{in}}\, dA \end{aligned} \tag{3.11}$$

Similarly the aerodynamic moment $\boldsymbol{g}$ about point O (see Fig. 2.3) assumes the form

$$\boldsymbol{g} = \rho V^2 \left[\frac{\sigma_t}{S} \mathcal{G}_1 \times \hat{\mathbf{v}} + \frac{2-\sigma_n}{S^2} \mathcal{G}_2 - \frac{\sigma_t}{S} \mathcal{G}_3 + \frac{\sigma_n}{S} \frac{V_w}{V} \mathcal{G}_4 \right] \tag{3.12}$$

where

$$\begin{aligned} \mathcal{G}_1 &= \iint \Gamma_1(S\cos\alpha)\, \mathbf{r}\, dA & \mathcal{G}_2 &= \iint \Gamma_2(S\cos\alpha)\, \mathbf{r} \times \mathbf{n}_{\text{in}}\, dA \\ \mathcal{G}_3 &= \iint \Gamma_1(S\cos\alpha)\cos\alpha\, \mathbf{r} \times \mathbf{n}_{\text{in}}\, dA & \mathcal{G}_4 &= \iint \Gamma_1(S\cos\alpha)\, \mathbf{r} \times \mathbf{n}_{\text{in}}\, dA \end{aligned} \tag{3.13}$$

In performing the surface integrals, recall that α is the angle between the surface unit inner normal $\mathbf{n}_{\text{in}}$ and mean flow velocity $\mathbf{V}$.

As remarked above, the hyperthermal flow assumption (which neglects the random motion of the atmospheric molecules) corresponds to an infinite value of the molecular speed ratio S. Recalling the limiting values of the error function: $\lim_{x \to \pm\infty} \mathrm{erf}(x) = \pm 1$, it is easy to show that

$$\begin{aligned} \lim_{S\to\infty} \left[1 + \mathrm{erf}(S\cos\alpha) \right] &= 2H(\cos\alpha) \\ \lim_{S\to\infty} \frac{\Gamma_1(S\cos\alpha)}{S} &= \cos\alpha\, H(\cos\alpha) \end{aligned} \tag{3.14}$$

From eqs.(3.6) & (3.8) it can be shown that

$$\Gamma_2(x) = x\Gamma_1(x) + \frac{1}{4}(1 + \mathrm{erf}\, x)$$

and hence

$$\lim_{S\to\infty} \frac{\Gamma_2(S\cos\alpha)}{S^2} = \cos^2\alpha\, H(\cos\alpha) \tag{3.15}$$

Armed with these results, it is readily demonstrated that in the limit of infinite S, eqs.(3.10) & (3.12) do indeed recover the hyperthermal results given by eqs.(2.10) &. (2.11).

3.2 Closed Form Solutions

Although the integrations are rather involved, we can obtain closed form solutions for the aerodynamic forces and torques for finite molecular speed ratio in the case of simple geometries. Below we present results for the a) Sphere, b) Flat Plate & c) Right Circular Cylinder. The force and moment components are plotted against angle of attack (except for the sphere) for selected values of the molecular speed ratio and are compared with the hyperthermal results. We demonstrate numerically, and prove analytically, that the resulting force and moment expressions reduce to the previously obtained hyperthermal results as the molecular speed ratio tends to infinity.

3.2.1 Sphere in Free-molecular Flow

Figure 2.4 shows a sphere of radius a with a system of spherical coordinates $\{r,\theta,\varphi\}$ at its center. Without loss of generality, we may assume that the incident mean molecular flow **V** is parallel to the z axis. The surface of the sphere is described by: $r=a$, $0\le\theta\le\pi$, $0\le\varphi\le 2\pi$ with element of surface area $dA = a^2\sin\theta\, d\theta\, d\varphi$. The unit inward normal is given by

$$\mathbf{n}_{in} = -\sin\theta\cos\mathbf{i} - \sin\theta\sin\varphi\,\mathbf{j} - \cos\theta\,\mathbf{k}$$

where **i**,**j**,**k** denote unit vectors along the axes of x,y,z respectively.

To evaluate the force associated surface integrals appearing in eq.(3.11) we make the substitution $x = -S\cos\theta$. The integration over φ is immediate and we find

$$\begin{aligned}
F_1 &= 2\pi a^2/S\int_{-S}^{S}\Gamma_1(x)dx\\
\mathcal{F}_4 &= 2\pi a^2/S^2\int_{-S}^{S}x\Gamma_1(x)dx\,\mathbf{k}\\
\mathcal{F}_3 &= 2\pi a^2/S^3\int_{-S}^{S}x^2\Gamma_1(x)dx\,\mathbf{k}\\
\mathcal{F}_2 &= 2\pi a^2/S^2\int_{-S}^{S}x\Gamma_2(x)dx\,\mathbf{k}
\end{aligned}$$

Utilizing integration by parts, we can perform the integration over x.

$$\begin{aligned}
\int_{-S}^{S}\Gamma_1(x)dx &= \frac{1}{4}\left(1+2S^2\right)\mathrm{erf}(S)+\frac{1}{2\sqrt{\pi}}Se^{-S^2}\\
\int_{-S}^{S}x\Gamma_1(x)dx &= \frac{1}{3}S^3\\
\int_{-S}^{S}x^2\Gamma_1(x)dx &= \frac{1}{16}\left(1+4S^4\right)\mathrm{erf}(S)+\frac{1}{8\sqrt{\pi}}\left(2S^2-1\right)Se^{-S^2}\\
\int_{-S}^{S}x\Gamma_2(x)dx &= \frac{1}{16}\left(4S^4+4S^2-1\right)\mathrm{erf}(S)+\frac{1}{8\sqrt{\pi}}\left(2S^2+1\right)Se^{-S^2}
\end{aligned}\qquad (3.16)$$

Combining the above results we find that the net force on the sphere is a drag with magnitude $\rho V^2\pi a^2\, C_D/2$ where the drag coefficient is given by

$$C_D = \frac{2-\sigma_n+\sigma_t}{2S^3}\left[\frac{4S^4+4S^2-1}{2S}\mathrm{erf}(S)+\frac{2S^2+1}{\sqrt{\pi}}e^{-S^2}\right]+\frac{4}{3}\sigma_n\frac{V_w}{V}\qquad (3.17)$$

Taking the limit of this expression as $S \to \infty$, we recover the hyperthermal result in eq.(2.13).

The drag coefficient is plotted below as a function of S with $\sigma_n=\sigma_t=0.7$ and $V_w/V=0.05$. Since the drag coefficient decreases with S, we conclude that the drag force is *underestimated* by the hyperthermal assumption.

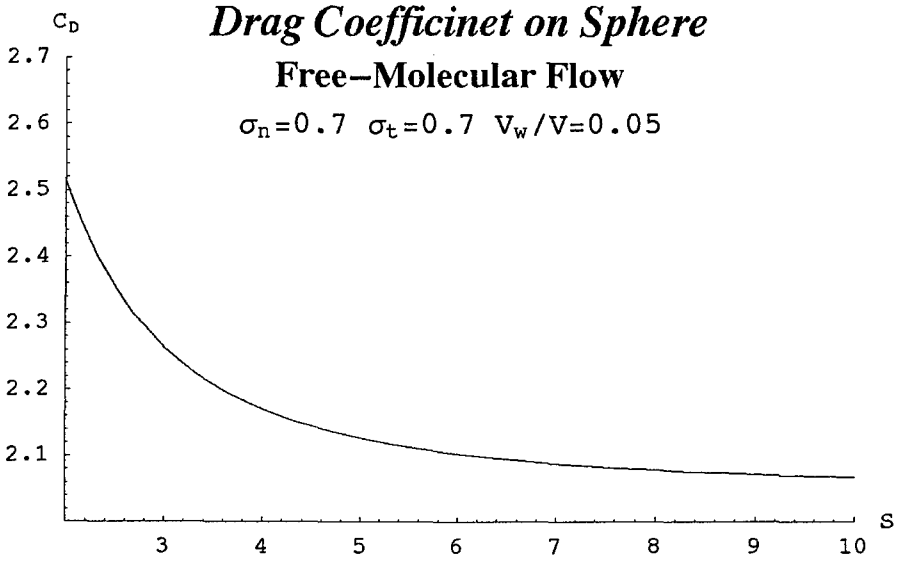

Figure 3.3 C_D for Sphere as a Function of S.

It is clear from symmetry (and verified by calculation) that the aerodynamic torque about the center of the sphere is zero.

3.2.2 Flat Plate in Free-molecular Flow

Figure 2.5 shows a flat plate of area A at angle of attack β with respect to the incident mean molecular velocity $\mathbf{V}$. A rectangular coordinate system is established with origin at the centroid of the plate with x,y axes respectively parallel and perpendicular to $\mathbf{V}$. In contrast to the prior hyperthermal analysis, the random motion of the molecules will result in impingement upon the back surface of the plate and hence we must now also integrate over that surface. Denote by S^+ and S^- the front and back surfaces (relative to $\mathbf{V}$) of the plate respectively. The angle α assumes constant values over the two surfaces, so the surface integrals are trivial to evaluate.

On S^+, $\cos\alpha = \sin\beta$ and the unit inward normal is given by $\mathbf{n} = \sin\beta\,\mathbf{i} + \cos\beta\,\mathbf{j}$. Denoting the contribution to the force (eq.) (3.10) by $\mathbf{f}^+$, we find

$$\mathbf{f}^+ = \frac{\rho V^2 A}{S}\left[\sigma_t\Gamma_1(S\sin\beta)\mathbf{i} + \frac{2-\sigma_n}{S}\Gamma_2(S\sin\beta)\mathbf{n} - \sigma_t\Gamma_1(S\sin\beta)\sin\beta\;\mathbf{n} + \sigma_n\frac{V_w}{V}\Gamma_1(S\sin\beta)\mathbf{n}\right]$$

On S^-, $\cos\alpha = -\sin\beta$ and the unit inward normal is $(-\mathbf{n})$. The corresponding force contribution $\mathbf{f}^-$ is given by

$$\mathbf{f}^- = \frac{\rho V^2 A}{S}\left[\sigma_t\Gamma_1(-S\sin\beta)\mathbf{i} - \frac{2-\sigma_n}{S}\Gamma_2(-S\sin\beta)\mathbf{n} - \sigma_t\Gamma_1(-S\sin\beta)\sin\beta\;\mathbf{n} - \sigma_n\frac{V_w}{V}\Gamma_1(-S\sin\beta)\mathbf{n}\right]$$

The following relations can be immediately verified and will prove useful in simplifying the expression for the net force on the plate (see eqs.(3.6) &(3.8).

$$\Gamma_1(x) + \Gamma_1(-x) = \frac{1}{\sqrt{\pi}}e^{-x^2} + x\,\mathrm{erf}(x)$$
$$\Gamma_1(x) - \Gamma_1(-x) = x$$
$$\Gamma_2(x) - \Gamma_2(-x) = \frac{1}{\sqrt{\pi}}xe^{-x^2} + \frac{1}{2}\left(1+2x^2\right)\mathrm{erf}(x)$$

Adding the two force components $\mathbf{f}^+$ and $\mathbf{f}^-$ and introducing the expression for the unit normal vector $\mathbf{n}$, we obtain the net force $\mathbf{f}$ on the plate in the form

$$\mathbf{f} = \frac{1}{2}\rho V^2 A\left(\mathrm{C}_D\,\mathbf{i} + \mathrm{C}_L\,\mathbf{j}\right)$$

where the lift and drag coefficients are given by

$$\mathrm{C}_L = \left[\frac{2-\sigma_n-\sigma_t}{\sqrt{\pi}S}\exp\left(-S^2\sin^2\beta\right) + \sigma_n\frac{V_w}{V}\right]\sin 2\beta + \left[\frac{2-\sigma_n}{S^2} + 2\left(2-\sigma_n-\sigma_t\right)\sin^2\beta\right]\cos\beta\,\mathrm{erf}\left(S\sin\beta\right) \tag{3.18}$$

$$C_D = 2\sigma_n \frac{V_w}{V}\sin^2\beta + \frac{2}{\sqrt{\pi}S}\left[(2-\sigma_n)\sin^2\beta + \sigma_t\cos^2\beta\right]\exp\left(-S^2\sin^2\beta\right) + 2\left[(2-\sigma_n)\left(\sin^2\beta + \frac{1}{2S^2}\right) + \sigma_t\cos^2\beta\right]\sin\beta\,\mathrm{erf}(S\sin\beta) \tag{3.19}$$

Taking the limit of the above expression as $S \to \infty$, we recover the hyperthermal results of eqs.(2.14) & (2.15).

It is readily shown that the aerodynamic moment about the centroid of the plate is zero.

The lift and drag coefficients are plotted below as functions of the angle of attack for $\sigma_n=\sigma_t=0.7$ and $V_w/V=0.05$. The solid curves correspond to $S=3$ while the dashed curves are the corresponding hyperthermal results. As in the hyperthermal case, the lift is antisymmetric about $\beta=\pi/2$ vanishing at $\beta=0,\pi/2$ and π. Note however that the angle of attack corresponding to maximum lift is affected by the molecular speed ratio. The drag remains symmetric about the point $\beta=\pi/2$ at which it is maximum; however it assumes a nonzero value at $\beta=0,\pi$ for finite S and $\sigma_t \neq 0$. We deduce from the plots that the magnitude of the aerodynamic force is *underestimated* by invoking the hyperthermal assumption.

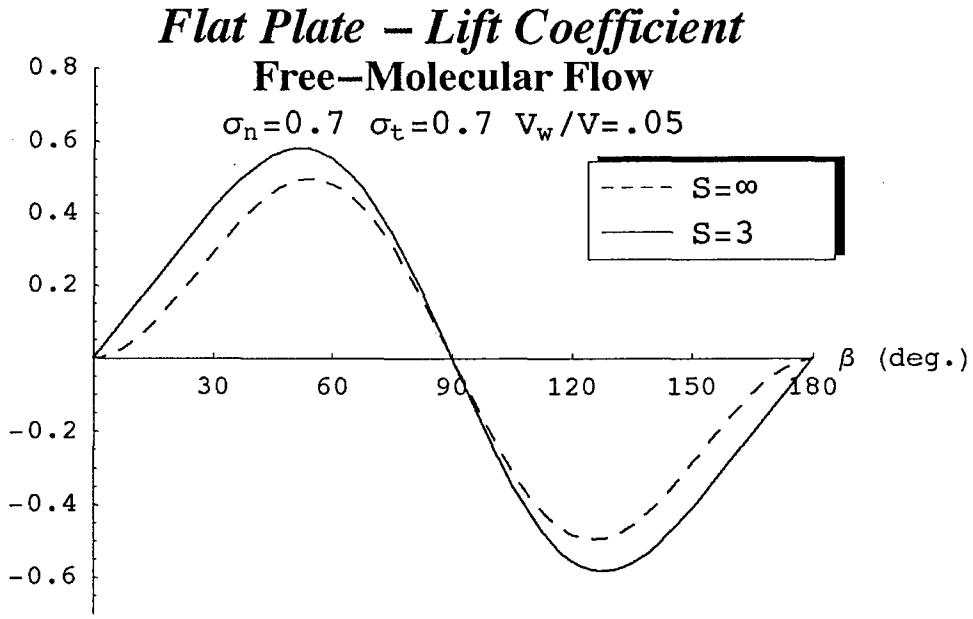

Figure 3.4. C_L for Flat Plate in Free-molecular Flow.

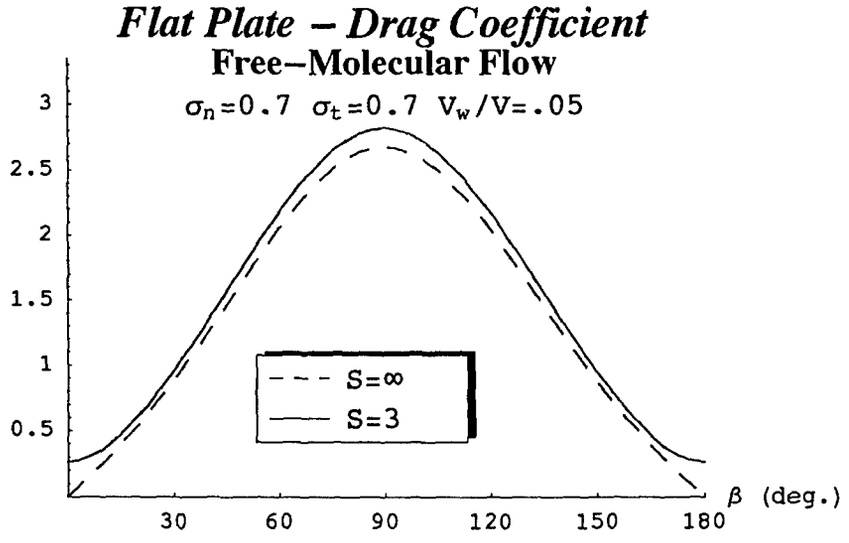

Figure 3.5. C_D for Flat Plate in Free-molecular Flow.

3.2.3 Right Circular Cylinder in Free-molecular Flow

We now calculate the aerodynamic force and torque on the cylinder shown in Figure 2.7 neglecting the effects of the two ends (these faces are simple flat plates which have been treated previously). The cylinder has length l and radius a while its axis is at an angle β with respect to the incident mean molecular velocity $\mathbf{V}$. As in the earlier hyperthermal analysis, it suffices to consider $0 \le \beta \le \pi/2$. A rectangular coordinate system with origin at the centroid O of the cylinder has its z axis along the axis of the cylinder and x axis in the plane determined by $\mathbf{V}$ and the cylinder axis. In terms of the cylindrical coordinates (r,θ,z), the lateral surface is described by $r = a, 0 \le \theta \le 2\pi, -l/2 \le z \le l/2$ and the element of surface area is given by $dA = a\,d\theta\,dz$. Observing that $\mathbf{n}_{in} = -\cos\theta\,\mathbf{i} - \sin\theta\,\mathbf{j}$ and $\hat{\mathbf{v}} = \sin\beta\,\mathbf{i} + \cos\beta\,\mathbf{k}$, we have $\cos\alpha = -\sin\beta\cos\theta$.

It follows from eq.(3.11) that

$$\mathcal{F}_1 = 2al\int_0^{\pi} \Gamma_1(\mu\cos\theta)d\theta \quad (\mu \equiv S\sin\beta)$$

Making the substitution $x = \mu\cos\theta$, and introducing eq.(3.6) we obtain

$$\mathcal{F}_1 = \frac{2al}{\sqrt{\pi}}\int_0^{\mu} \frac{e^{-x^2} + \sqrt{\pi}x\,\mathrm{erf}(x)}{\sqrt{\mu^2 - x^2}}dx$$

Performing the integrations, we obtain

$$\mathcal{F}_1 = \sqrt{\pi}al\,e^{-\mu^2/2}\left[(1+\mu^2)I_0(\mu^2/2) + \mu^2 I_1(\mu^2/2)\right] \tag{3.20}$$

where $I_\nu(\ )$ denotes the modified Bessel function of the first kind of order ν.

In a similar fashion (introducing eq.(3.8)),it can be shown that

$$\mathcal{F}_2 = 2al\int_0^{\pi} \Gamma_2(\mu\cos\theta)\cos\theta\, d\theta\, \mathbf{i} = \frac{2al}{\sqrt{\pi}\mu}\int_0^{\mu} \frac{x^2 e^{-x^2} + \sqrt{\pi}/2\left(x+2x^3\right)\operatorname{erf} x}{\sqrt{\mu^2 - x^2}}\, dx\, \mathbf{i}$$

Performing the integrations, we find

$$\mathcal{F}_2 = \frac{\sqrt{\pi}}{3} al\mu e^{-\mu^2/2}\left[\left(2\mu^2+3\right)I_0\left(\mu^2/2\right) + \left(2\mu^2+1\right)I_1\left(\mu^2/2\right)\right]\mathbf{i} \tag{3.21}$$

Likewise,

$$\mathcal{F}_3 = 2al\mu/S\int_0^{\pi} \Gamma_1(\mu\cos\theta)\cos^2\theta\, d\theta\, \mathbf{i} = \frac{2al}{\mu S}\int_0^{\mu} \frac{x^2}{\sqrt{\mu^2 - x^2}}\left(\frac{1}{\sqrt{\pi}} e^{-x^2} + x\operatorname{erf} x\right) dx\, \mathbf{i}$$

Performing the integrations, we obtain

$$\mathcal{F}_3 = \frac{\sqrt{\pi}}{6} al\,\mu/S e^{-\mu^2/2}\left[\left(3+4\mu^2\right)I_0\left(\mu^2/2\right) + \left(4\mu^2-1\right)I_1\left(\mu^2/2\right)\right]\mathbf{i} \tag{3.22}$$

Finally,

$$\mathcal{F}_4 = 2al\int_0^{\pi} \Gamma_1(\mu\cos\theta)\cos\theta\, d\theta\, \mathbf{i} = \frac{2al}{\mu}\int_0^{\mu} \frac{x^2}{\sqrt{\mu^2 - x^2}}\, dx\, \mathbf{i} = \frac{\pi}{2} al\mu\ \mathbf{i} \tag{3.23}$$

Inserting the expressions from eqs.(3.20)–(3.23) into eq.(3.10) yields the aerodynamic force on the lateral surface with components f_x and f_z given by

$$f_x = \rho V^2 al\left\{\frac{\pi}{2}\sigma_n \frac{V_w}{V}\sin\beta - \frac{\sqrt{\pi}}{6}\left(2\sigma_n - \sigma_t - 4\right)\frac{e^{-\mu^2/2}}{\mu}\sin^2\beta\left[\left(2\mu^2+3\right)I_0\left(\mu^2/2\right) + \left(2\mu^2+1\right)I_1\left(\mu^2/2\right)\right]\right\}$$

$$f_z = \sqrt{\pi}\rho V^2 al\,\sigma_t\,\mu^{-1}\sin\beta\cos\beta\, e^{-\mu^2/2}\left[\left(1+\mu^2\right)I_0\left(\mu^2/2\right) + \mu^2 I_1\left(\mu^2/2\right)\right] \tag{3.24}$$

Recalling that $\mu = S\sin\beta$, we should recover the hyperthermal result derived earlier by taking the limit of the above expressions as $\mu \to \infty$. Utilizing the asymptotic expansions for the Modified Bessel functions

$$I_0(\lambda) \sim I_1(\lambda) \sim \frac{e^{\lambda}}{\sqrt{2\pi\lambda}}$$

we find

$$\lim_{\mu\to\infty} \frac{\left(2\mu^2+3\right)I_0\left(\mu^2/2\right) + \left(2\mu^2+1\right)I_1\left(\mu^2/2\right)}{\mu e^{\mu^2/2}} = \frac{4}{\sqrt{\pi}}$$

$$\lim_{\mu\to\infty} \frac{\left(\mu^2+1\right)I_0\left(\mu^2/2\right) + \mu^2 I_1\left(\mu^2/2\right)}{\mu e^{\mu^2/2}} = \frac{2}{\sqrt{\pi}}$$

Thus the limiting value of the forces in eq.(3.24) as $S \to \infty$ do indeed degenerate to those given in eq. (2.16).

The axial and transverse forces (f_z,f_x) on the lateral surface of the cylinder are plotted in Fig. 3.6 as a function of the angle of attack (for σ_n=σ_t=0.7 and V_w/V=0.05) with the solid curves corresponding to eq.(3.24) with S=3 and the dashed curves indicating the corresponding hyperthermal result as given by eq.(2.16). In both cases, f_x vanishes at $\beta = 0$ and attains its maximum value at $\beta = \pi/2$. We note however that at $\beta = 0$, f_z is non zero for a finite speed ratio $(\sigma_t \neq 0)$ while it is zero in the hyperthermal limit. A similar result was observed in the previous case of the flat plate. Again, the plots show that the magnitudes of the aerodynamic forces are underestimated by invoking the hyperthermal assumption.

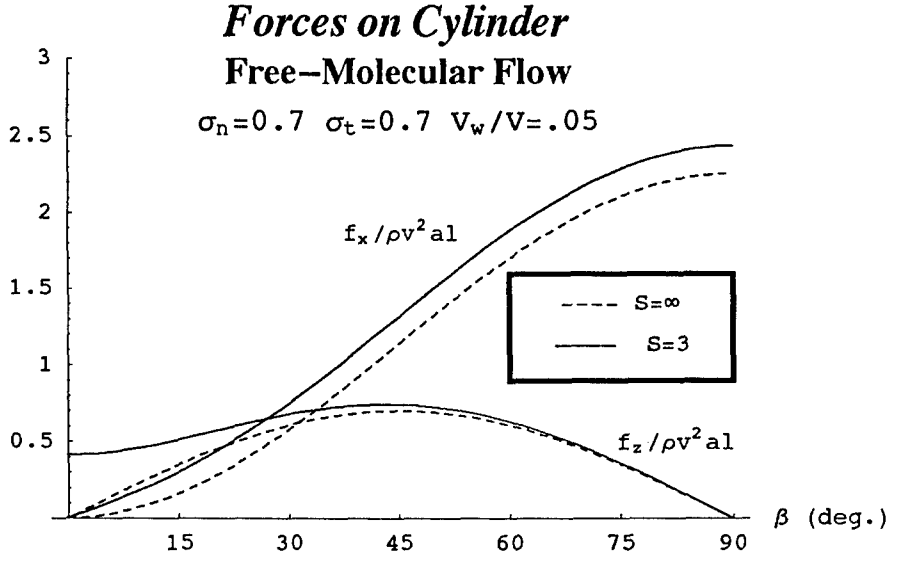

Figure 3.6. Forces on Lateral Surface of Cylinder in Free-molecular Flow

To calculate the aerodynamic torque, we need to evaluate the four integrals in eq.(3.13). It is readily shown that the integrals $\mathcal{G}_2$,$\mathcal{G}_3$ and $\mathcal{G}_4$ all vanish. The remaining integral is simply related to the above value of $\mathcal{F}_4$.

$$\mathcal{G}_1 = -a\mathcal{F}_4 = -\frac{\pi}{2}a^2 l\mu \mathbf{i} \tag{3.25}$$

The aerodynamic moment about the centroid of the cylinder then follows from eq.(3.12)

$$\mathbf{g} = \frac{\pi}{4}a^2 l\rho V^2 \sigma_t \sin 2\beta \, \mathbf{j} \tag{3.26}$$

Interestingly, the moment unlike the force, is independent of the molecular speed ratio and of course agrees with the hyperthermal result given in eq.(2.17).

4. Rotating Axisymmetric Bodies in Hyperthermal Free-molecular Flow

So far in our investigation, the bodies under consideration were not rotating with respect to the oncoming (mean) flow and hence the surface relative velocity of the incident molecules did not vary over the impinged surface area. We now consider the general class of axisymmetric convex bodies which are rotating about their axis of symmetry but have arbitrary orientation relative to the incident molecular flux. In order not to obfuscate the effects of rotation, we restrict our attention to the case of a hyperthermal free-molecular flow; this assumption is removed in the subsequent section. General expressions in terms of definite integrals are obtained for the aerodynamic force and moment resolved along a set of space fixed axes. The quadratures are carried through explicitly for some simple geometries and force and moment components which arise from the body's rotation are plotted against the incident angle of attack.

4.1 Surface Geometry

Figure 4.1 shows a body rotating about its axis of symmetry at rate ω relative to the atmosphere. We define a spatially-fixed coordinate system $\{x,y,z\}$ with corresponding unit vectors **i**, **j**, and **k** taking the z axis along the axis of symmetry. The incident molecules have velocity $\mathbf{V}_0$ relative to the origin O where $\mathbf{V}_0$ is at an angle β with respect to the $-z$ axis and is taken (without loss of generality) to lie in the y-z plane. At the element of surface area dA instantaneously at point $\boldsymbol{r}$, we construct a body fixed frame with unit vectors$\{\mathbf{t},\mathbf{n},\mathbf{b}\}$ along the local tangent, normal and binormal directions i.e. **t** is along $\boldsymbol{\omega}\times\boldsymbol{r}$, **n** points in the direction of the inner normal to the surface, and $\mathbf{b}=\mathbf{t}\times\mathbf{n}$. It proves convenient to introduce cylindrical coordinates $\{\bar{\rho},\varphi,z\}$ related to the rectangular coordinates by

$$x=\bar{\rho}\sin\varphi,\quad y=-\bar{\rho}\cos\varphi \tag{4.1}$$

Note that since the flow is symmetric with respect to the y-z plane, this choice of φ will render many expressions to be even functions of φ thus simplifying the integration. Since the z axis is an axis of symmetry, $\bar{\rho}$ will be a prescribed function of z on the surface. The position vector $\boldsymbol{r}$ to a point on the surface is given by the expression

$$\boldsymbol{r}(z,\varphi)=\bar{\rho}\sin\varphi\,\mathbf{i}-\bar{\rho}\cos\varphi\,\mathbf{j}+z\,\mathbf{k} \tag{4.2}$$

The unit vectors **t** and **b** are along the directions of $\partial\boldsymbol{r}/\partial\varphi$ and $\partial\boldsymbol{r}/\partial z$ respectively, while $\mathbf{n}=\mathbf{b}\times\mathbf{t}$. If we define θ as the angle between the *outer* normal to the surface and the z axis, we can write

$$\begin{aligned}\mathbf{t}&=\cos\varphi\,\mathbf{i}+\sin\varphi\,\mathbf{j}\\ \mathbf{b}&=-\cos\theta\sin\varphi\,\mathbf{i}+\cos\theta\cos\varphi\,\mathbf{j}+\sin\theta\,\mathbf{k}\\ \mathbf{n}&=-\sin\varphi\sin\theta\,\mathbf{i}+\cos\varphi\sin\theta\,\mathbf{j}-\cos\theta\,\mathbf{k}\end{aligned} \tag{4.3}$$

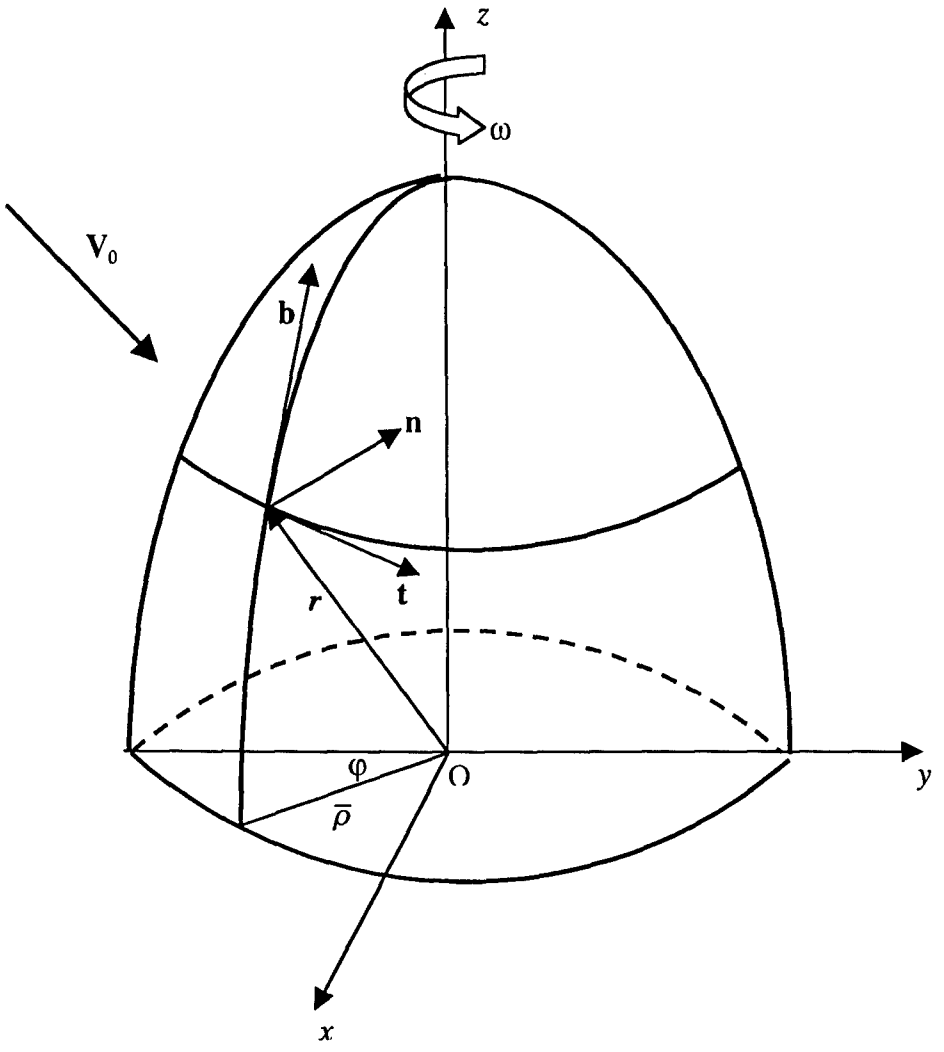

Figure 4.1. Axisymmetric Body in Free-molecular Flow

Thus the transformation matrix **T** from the {**n**,**b**,**t**} to the {**i**,**j**,**k**} basis can be expressed as

$$\mathbf{T} = \begin{pmatrix} -\sin\theta\sin\varphi & -\cos\theta\sin\varphi & \cos\varphi \\ \sin\theta\cos\varphi & \cos\theta\cos\varphi & \sin\varphi \\ -\cos\theta & \sin\theta & 0 \end{pmatrix} \tag{4.4}$$

The element of surface area is given by $dA = \|\partial r/\partial\varphi \times \partial r/\partial z \, d\varphi \, dz\|$ which can be expressed in the form

$$dA = \bar{\rho} \csc\theta \, d\varphi \, dz \tag{4.5}$$

The velocity **V** of the incident molecules relative to the surface is given by

$$\mathbf{V} = \mathbf{V}_0 - \boldsymbol{\omega} \times \boldsymbol{r}$$

In contrast to the non-rotating case, the surface relative velocity now varies over the surface. Expressed in the surface-fixed triad, we obtain

$$\begin{aligned} \mathbf{V} = {} & V_0(\cos\beta\cos\theta + \sin\beta\cos\varphi\sin\theta)\mathbf{n} + V_0(\sin\beta\cos\theta\cos\varphi - \cos\beta\sin\theta)\mathbf{b} \\ & + (V_0 \sin\beta\sin\varphi - \bar{\rho}\omega)\mathbf{t} \end{aligned} \tag{4.6}$$

To a high degree of approximation, we can replace ω with the body's inertial angular velocity. As discussed in Sec. 2.2, it is important to limit the aerodynamic pressure to those portions of the surface which actually are impinged by the atmospheric molecuules. This requirement may be expressed by the inequality $\mathbf{V}\cdot\mathbf{n} > 0$. To effect this limitation, we will insert the factor $H(\eta)$ into the surface integrals of the aerodynamic forces and torques to be derived below where

$$\eta = \cos\beta\cos\theta + \cos\varphi\sin\beta\sin\theta \tag{4.7}$$

4.2 Aerodynamic Forces & Moments

As shown in Sec. 2.2, the incident flow has an associated mass flux of $\rho\mathbf{V}\cdot\mathbf{n}$ and momentum flux of $\rho(\mathbf{V}\cdot\mathbf{n})\mathbf{V}$. Denoting by p_{ni}, p_{bi}, p_{ti} the components of the incident momentum flux along the local normal, binormal and tangent directions, we obtain

$$\begin{aligned} p_{ni} &= \rho V_0^2 \, \eta^2 \\ p_{bi} &= \rho V_0^2 \eta(\cos\theta\cos\varphi\sin\beta - \cos\beta\sin\theta) \\ p_{ti} &= \rho V_0 \, \eta(V_0 \sin\varphi\sin\beta - \bar{\rho}\omega) \end{aligned} \tag{4.8}$$

In addition to the above incident momentum flux, we require an expression for p_w – the normal component of momentum flux which would be carried away from the surface by diffusely reflected molecules in thermal equilibrium with the surface. Utilizing the above expression for the mass flux, we obtain

$$p_w = \rho V_0 \eta \, V_w \tag{4.9}$$

where V_w is given by eq.(2.3). From the definitions of the momentum accommodation coefficients (eq.(2.1)), we can calculate the reflected momentum flux in terms of the incident momentum flux, p_w, σ_n and σ_t. Subtracting the reflected from the incident momentum flux yields the force per unit area, $\boldsymbol{P}$, exerted by the molecules upon the surface.

$$\begin{aligned} & \boldsymbol{P} = P_n \mathbf{n} + P_b \mathbf{b} + P_t \mathbf{t} \\ & \text{where } P_n = (2 - \sigma_n)p_{ni} + \sigma_n p_w, \; P_b = \sigma_t p_{bi}, \; P_t = \sigma_t p_{ti} \end{aligned} \tag{4.10}$$

With the aid of eq.(4.3), we can now calculate the net force $\boldsymbol{F}$ on the body resolved along the axes of the fixed $\{x,y,z\}$ coordinate system.

$$\begin{aligned} F_x &= \oiint \left[P_t \cos\varphi - P_n \sin\theta \sin\varphi - P_b \cos\theta \sin\varphi \right] H(\eta)\, dA \\ F_y &= \oiint \left[P_t \sin\varphi + P_n \sin\theta \cos\varphi + P_b \cos\theta \cos\varphi \right] H(\eta)\, dA \\ F_z &= \oiint \left[P_b \sin\theta - P_n \cos\theta \right] H(\eta)\, dA \end{aligned} \tag{4.11}$$

In a similar fashion, the aerodynamic moment $\boldsymbol{M}$ about the $\{x,y,z\}$ origin can be calculated with the aid of eqs.(4.2), (4.3)& (4.10)

$$\begin{aligned} M_x &= \oiint \left[\cos\varphi \left(\bar{\rho}\cos\theta - z\sin\theta \right) P_n - \cos\varphi \left(z\cos\theta + \bar{\rho}\sin\theta \right) P_b - z\sin\varphi\, P_t \right] H(\eta)\, dA \\ M_y &= \oiint \left[\left(\bar{\rho}\cos\theta - z\sin\theta \right) \sin\varphi\, P_n - \left(z\cos\theta + \bar{\rho}\sin\theta \right) \sin\varphi\, P_b + z\cos\varphi\, P_t \right] H(\eta)\, dA \\ M_z &= \oiint \bar{\rho}\, P_t\, H(\eta)\, dA \end{aligned} \tag{4.12}$$

The force and moment expressions given above are in a form suitable for numerical implementation.

We now proceed to expand the above force and moment expressions so as to reveal in an explicit manner the effects of body rotation upon these aerodynamic disturbances. Due to symmetry, many simplifications will occur in the process of generating the final formulas thus allowing for closed form solutions to several geometric primitives.

Combining eqs.(4.8)–(4.10) we obtain

$$\begin{aligned} P_n &= \left(2 - \sigma_n \right) \rho V_0^2\, \eta^2 + \sigma_n \rho V_0 V_w \eta \\ P_b &= \sigma_t \rho V_0^2 \eta \left(\cos\theta \cos\varphi \sin\beta - \cos\beta \sin\theta \right) \\ P_t &= \sigma_t \rho V_0 \eta \left(V_0 \sin\varphi \sin\beta - \bar{\rho}\omega \right) \end{aligned} \tag{4.13}$$

We make the following observations

1) $\bar{\rho}$ and θ are independent of φ

2) η is an even function of φ

3) P_n and P_b are even functions of φ

4) P_t is the sum of an even and odd function of φ

The region of integration is described by: $\{-\pi < \varphi < \pi;\, z_1 < z < z_2\}$ and the element of surface area is given by eq.(4.5). In light of the above observations, we can express the force components in the form

$$F_x = -2\sigma_t \rho V_0 \omega \int_{z_1}^{z_2}\int_0^{\pi} \overline{\rho}^2 \csc\theta \cos\varphi\, \eta\, H(\eta)\, d\varphi\, dz$$

$$F_y = 2\rho V_0^2 \int_{z_1}^{z_2}\int_0^{\pi} [\sin\theta\cos\varphi\left((2-\sigma_n)\eta + \sigma_n V_w/V_0\right) + \sigma_t \cos\theta\cos\varphi\left(\sin\beta\cos\theta\cos\varphi - \cos\beta\sin\theta\right) + \sigma_t \sin\beta\sin^2\varphi\,]\, \eta\, H(\eta)\overline{\rho}\csc\theta\, d\varphi\, dz \tag{4.14}$$

$$F_z = 2\rho V_0^2 \int_{z_1}^{z_2}\int_0^{\pi} [\sigma_t \sin\theta\left(\sin\beta\cos\varphi\cos\theta - \cos\beta\sin\theta\right) - \cos\theta\left((2-\sigma_n)\eta + \sigma_n V_w/V_0\right)]\, \eta\, H(\eta)\overline{\rho}\csc\theta\, d\varphi\, dz$$

In a similar fashion, the components of the moment can be reduced to

$$M_x = 2\rho V_0^2 \int_{z_1}^{z_2}\int_0^{\pi} [\cos\varphi\left(\overline{\rho}\cos\theta - z\sin\theta\right)\left((2-\sigma_n)\eta + \sigma_n V_w/V_0\right) - \sigma_t \cos\varphi\left(z\cos\theta + \overline{\rho}\sin\theta\right)\left(\cos\theta\cos\varphi\sin\beta - \cos\beta\sin\theta\right) - \sigma_t z\sin\beta\sin^2\varphi\,]\eta\, H(\eta)\overline{\rho}\csc\theta\, d\varphi\, dz \tag{4.15}$$

$$M_y = -2\sigma_t \rho V_0 \omega \int_{z_1}^{z_2}\int_0^{\pi} z\,\overline{\rho}^2 \cos\varphi\, \eta\, H(\eta)\csc\theta\, d\varphi\, dz$$

$$M_z = -2\sigma_t \rho V_0 \omega \int_{z_1}^{z_2}\int_0^{\pi} \overline{\rho}^3 \eta\, H(\eta)\csc\theta\, d\varphi\, dz$$

We observe that the body's rotation has no affect on F_y, F_z and M_x but introduces additional disturbances F_x, M_y and M_z proportional to the body's angular rate. It is interesting to note that the lift force, F_x, acts in opposite direction to that which would obtain under a continuum flow (Magnus effect) i.e. we can show that the lift force corresponding to a free-molecular flow acts in the direction of $\boldsymbol{\omega}\times\mathbf{V}_0$. Taking $\omega > 0$, we will thus show that $F_x < 0$. Based upon eq.(4.14), we must prove that

$$\int_{z_1}^{z_2} \overline{\rho}^2 \csc\theta \int_0^{\pi} \cos\varphi\, \eta\, H(\eta) d\varphi\, dz \geq 0$$

Since $\theta, \beta \in (0,\pi)$, $\sin\beta \geq 0$ and $\sin\theta \geq 0$. It is therefore sufficient to demonstrate that the inner integral is nonnegative. From eq.(4.7), we can write $\eta = a\cos\varphi + c$; $a = \sin\beta\sin\theta \geq 0$, and $c = \cos\beta\cos\theta$. It is easy to show that

$$\int_0^{\pi} \cos\varphi\, \eta\, H(\eta) d\varphi = \int_0^{\pi/2} \left[\left(a\cos\varphi + c\right)H\left(a\cos\varphi + c\right) - \left(-a\cos\varphi + c\right)H\left(-a\cos\varphi + c\right)\right]\cos\varphi\, d\varphi$$

For $0 \leq \varphi \leq \pi/2$, $a\cos\varphi + c \geq -a\cos\varphi + c$; and of course $H(\,)$ is a monotonically increasing function of its argument. It follows that $\int_0^{\pi} \cos\varphi\, \eta\, H(\eta) d\varphi \geq 0$ *(QED)*

4.3 Closed Form Solutions

We provide below closed form expressions for the aerodynamic forces and moments on a circular disk, sphere, right circular cylinder and right circular cone where each body rotates about its axis of symmetry. Since results for the non-rotating case have been provided in Sec. 2.3, we shall only consider disturbances arising from body rotation.

4.3.1 Spinning Disk in Hyperthermal Free-molecular Flow

Consider the disk $x^2+y^2 \le R^2$ lying in the plane z=0. Restricting the angle of attack to $0 \le \beta \le \pi/2$, we have impingement only on the top surface $(\theta = 0)$ where $\eta = \cos\beta$ (see eq.(4.7)). The element of surface area is given by $dA = \bar{\rho}\, d\bar{\rho}\, d\varphi$. Due to the degenerate nature of this surface, we need to modify the form of the integrals given in eqs.(4.14) &. (4.15). The region of integration will be $\{0 \le \bar{\rho} \le R; 0 \le \varphi \le 2\pi\}$ (recall that advantage was taken of symmetry in eqs. (4.14)&;(4.15) thus the factor of 2 and integration over $0 \le \varphi \le \pi$).

$$F_x(\omega) = -\sigma_t \rho V_0 \omega \cos\beta \int_0^{2\pi}\int_0^R \bar{\rho}^2 \cos\varphi\, d\bar{\rho}\, d\varphi = 0$$

$$M_y(\omega) = 0$$

$$M_z(\omega) = -\sigma_t \rho V_0 \omega \cos\beta \int_0^{2\pi}\int_0^R \bar{\rho}^3 d\bar{\rho}\, d\varphi = -\frac{\pi}{2}\sigma_t \rho V_0 R^4 \omega \cos\beta$$

Thus rotation has no affect upon the force and produces a torque opposing the direction of spin.

4.3.2 Spinning Sphere in Hyperthermal Free-molecular Flow

Figure 4.2 shows a sphere of radius R rotating about the z axis with angular rate ω. The hemispherical portion of the sphere impinged by the oncoming flow (incident at angle β with respect to the z axis) is not conveniently described by the set of cylindrical coordinates $\{\bar{\rho}, \varphi, z\}$ defined in Figure 4.1. We therefore transform to a new rectangular coordinate system $\{X, Y, Z\}$ by rotating about the x axis by angle β. A set of spherical coordinates $\{R, \Theta, \Phi\}$ at the center of the sphere is defined by the transformations

$$X = R\sin\Theta\sin\Phi, \quad Y = -R\sin\Theta\cos\Phi, \quad Z = R\cos\Theta \tag{4.16}$$

The element of surface area is given by $dA = R^2 \sin\Theta\, d\Theta\, d\Phi$ and the region of integration (impinged portion of surface) is conveniently described by $\{-\pi < \Phi < \pi; 0 < \Theta < \pi/2\}$. In order to apply the general formulas given by eqs.(4.14)&(4.15), we need to relate the cylindrical coordinates $\{\bar{\rho}, \varphi, z\}$ to the spherical coordinates $\{R, \Theta, \Phi\}$. The transformation between the two sets of rectangular coordinates is given by

$$(x, y, z) = (X, \cos\beta\, Y - \sin\beta\, Z, \sin\beta\, Y + \cos\beta\, Z)$$

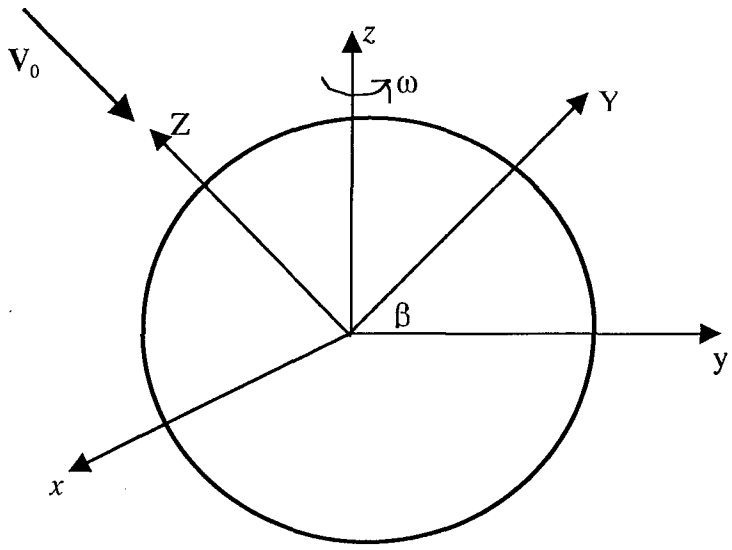

Figure 4.2. Rotating Sphere in Free-molecular Flow

Introducing eqs.(4.1) & (4.16) into the above, we obtain the relations

$$\begin{aligned} \bar{\rho}\sin\varphi &= R\sin\Theta\sin\Phi \\ \bar{\rho}\cos\varphi &= R\left(\sin\beta\cos\Theta+\cos\beta\sin\Theta\cos\Phi\right) \\ z &= R\left(\cos\beta\cos\Theta-\sin\beta\sin\Theta\cos\Phi\right) \end{aligned} \tag{4.17}$$

Recalling the definition of θ, we see that for the present case of the sphere, $\cos\theta = z/R$ and $\sin\theta = \bar{\rho}/R$. Utilizing these results in eq.(4.7), we obtain, as expected, $\eta = \cos\Theta$. The flow being symmetric with respect to the *y*-*z* plane implies that all integrands in eqs.(4.14) & (4.15) are even functions of Φ. Performing the integrations, we obtain.

$$\begin{aligned} F_x(\omega) &= -\frac{2\pi}{3}\sigma_t\rho V_0 R^3\omega\sin\beta \\ M_y(\omega) &= -\frac{\pi}{8}\sigma_t\rho V_0 R^4\omega\sin 2\beta \\ M_z(\omega) &= -\frac{\pi}{8}\sigma_t\rho V_0 R^4\omega\left(5-\cos 2\beta\right) \end{aligned} \tag{4.18}$$

The two torque components (scaled by $\pi\sigma_t\rho V_0 R^4\omega/8$) are plotted below as functions of the angle of attack. Note that the rotation of the sphere results in a torque opposing the spin direction over the entire range of angle of attack.

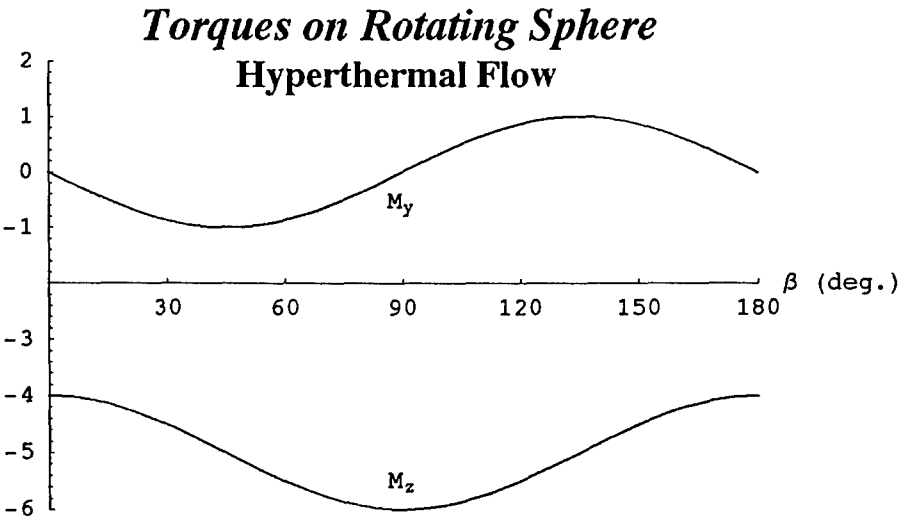

Figure 4.3. Spin Moments on Sphere in Hyperthermal Free-molecular Flow

4.3.3 Spinning Cylinder in Hyperthermal Free-molecular Flow

With reference to Fig. 4.1, a right circular cylinder of radius R and length L has its centroid at the origin of the Cartesian coordinate system $\{x, y, z\}$. The cylinder is rotating about its axis (z) at angular rate ω with an impinging free-molecular flow incident at angle of attack β. On the lateral surface of the cylinder, $\theta = \pi/2$, $\eta = \sin\beta\cos\varphi$ and for $0 < \beta < \pi$, $\eta > 0$ if $|\varphi| < \pi/2$. It follows from eqs.(4.14) & (4.15) that the spin induces a force on this portion of the surface given by

$$F_x^l = -\frac{\pi}{2}\omega\sigma_t\rho V_0 R^2 L\sin\beta$$

and a moment about the center of the cylinder

$$M_y^l = 0$$
$$M_z^l = -2\omega\sigma_t\rho V_0 R^3 L\sin\beta$$

If we restrict $0 \le \beta < \pi/2$, then there will be no impingement on the bottom surface $(z = -L/2)$of the cylinder. The force and moment on the top portion of the cylinder follow from the analysis above of the spinning disk. Thus the *net* force and moment on the cylinder due to its rotation are given by

$$
\begin{aligned}
F_x(\omega) &= -\frac{\pi}{2}\omega\sigma_t\rho V_0 R^2 L\sin\beta \\
M_y(\omega) &= 0 \\
M_z(\omega) &= -\frac{1}{2}\omega\sigma_t\rho V_0 R^3\left(\pi R\cos\beta + 4L\sin\beta\right)
\end{aligned}
\tag{4.19}
$$

The z component of the moment (scaled by $-\omega\sigma_t\rho V_0 R^3/2$) is plotted below as a function of the angle of attack for i) R=1,L=5 and ii) R=5,L=1.

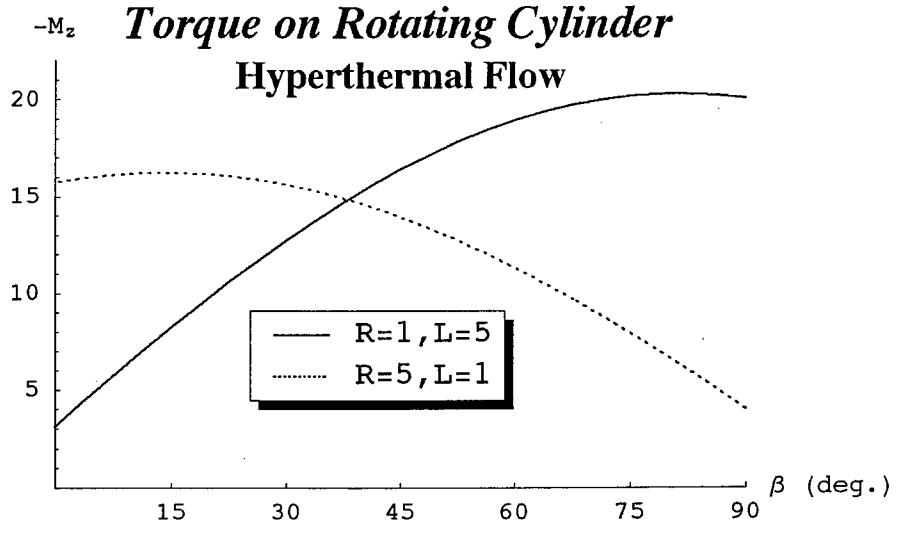

Figure 4.4. Spin Moments on Cylinder in Hyperthermal Free-molecular Flow

4.3.4 Spinning Cone in Hyperthermal Free-molecular Flow

Figure 4.5 shows a right circular cone of base radius R and height L with the origin of the Cartesian coordinate system $\{x,y,z\}$ at the center of its base. The cone is rotating about its axis (z) at angular rate ω with an incident free molecular flow $\mathbf{V}_0$ at angle of attack β. We restrict β to the range $(0,\pi/2)$ so that there will be no impingement on the base of the cone. The angle θ between the outer normal to the surface and the z axis is given by $\theta=\pi/2-\gamma$ where γ is the half-angle of the cone i.e. $\tan\gamma = R/L$. The cylindrical coordinate $\overline{\rho}$ is given by $\overline{\rho}=(L-z)\tan\gamma$, and from eq.(4.7), $\eta=\cos\beta\sin\gamma+\sin\beta\cos\gamma\cos\varphi$. To determine when η is positive, it proves convenient to consider the two cases 1) $0\le\beta<\gamma$ and 2) $\gamma<\beta\le\pi/2$.

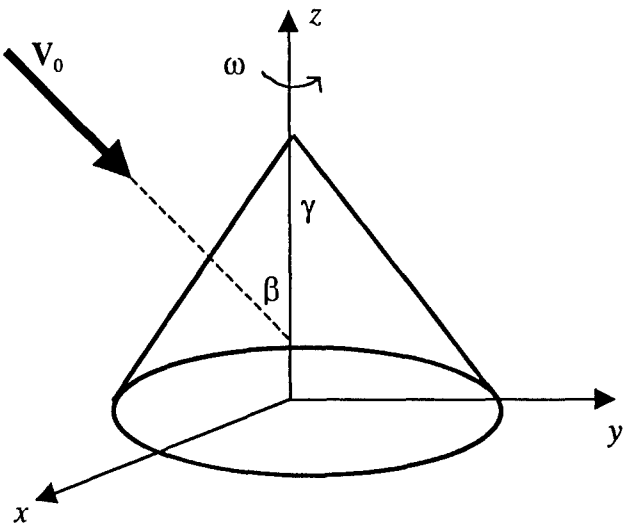

Figure 4.5. Rotating Cone in Free-molecular Flow

• Case 1. $0 \le \beta < \gamma$

Here we will have $\sin\beta < \sin\gamma$ and $\cos\beta > \cos\gamma$ so that $\cos\beta\sin\gamma > \cos\gamma\sin\beta > 0$ and hence $\eta > 0$ for all φ. Performing the integration in eqs.(4.14) & (4.15) we obtain

$$\begin{aligned} F_x(\omega) &= -\frac{\pi}{3}\sigma_t \rho V_0 R^3 \cot\gamma\, \omega \sin\beta \\ M_y(\omega) &= \frac{1}{4} R \cot\gamma\, F_x(\omega) \\ M_z(\omega) &= -\frac{\pi}{2}\sigma_t \rho V_0 R^4 \omega \cos\beta \end{aligned} \tag{4.20}$$

• Case 2. $\gamma < \beta \le \pi/2$

In this case, $\cos\beta < \cos\gamma$ and $\sin\gamma < \sin\beta$ therefore η is positive at $\varphi = 0$ and negative at $\varphi = \pi$. It can be shown that $\eta(\varphi)$ has a single root on $[0,\pi]$ at $\varphi = \varphi^*$ where

$$\varphi^* = \cos^{-1}\left(-\frac{\tan\gamma}{\tan\beta}\right)$$

Hence the integration limits are now $\{0 \le z \le L; 0 \le \varphi \le \varphi^*\}$. Since $\lim_{\beta \to \gamma^+} \varphi^* = \pi$, we will have a continuous transition across the point β=γ. Performing the integration in eqs. (4.14)&(4.15) we obtain

$$\begin{aligned} F_x(\omega) &= -\frac{1}{3}\sigma_t \rho V_0 R^3 \omega \left(\varphi^* \sin\beta \cot\gamma + \cos\beta \sin\varphi^*\right) \\ M_y(\omega) &= \frac{R}{4}\cot\gamma \, F_x(\omega) \\ M_z(\omega) &= -\frac{1}{2}\sigma_t \rho V_0 R^4 \omega \left(\varphi^* \cos\beta + \cot\gamma \sin\beta \sin\varphi^*\right) \end{aligned} \tag{4.21}$$

Fig. 4.6 is a plot of the spin induced force $F_x(\omega)$ (scaled by $-\sigma_t \rho V_0 R^3 \omega / 3$) as a function of the angle of attack for a cone with half-angle of 30°. It is interesting to note that the magnitude of this force starts out as an increasing function of the angle of attack (β) but does *not* assume its maximum value at $\beta = 90^\circ$.

The spin induced torques $M_y(\omega)$ and $M_z(\omega)$ (scaled by $-\sigma_t \rho V_0 R^4 \omega$) are shown in Fig. 4.7 as functions of the angle of attack on the 30° cone. We note that the magnitude of M_z is significantly larger than that of M_y.

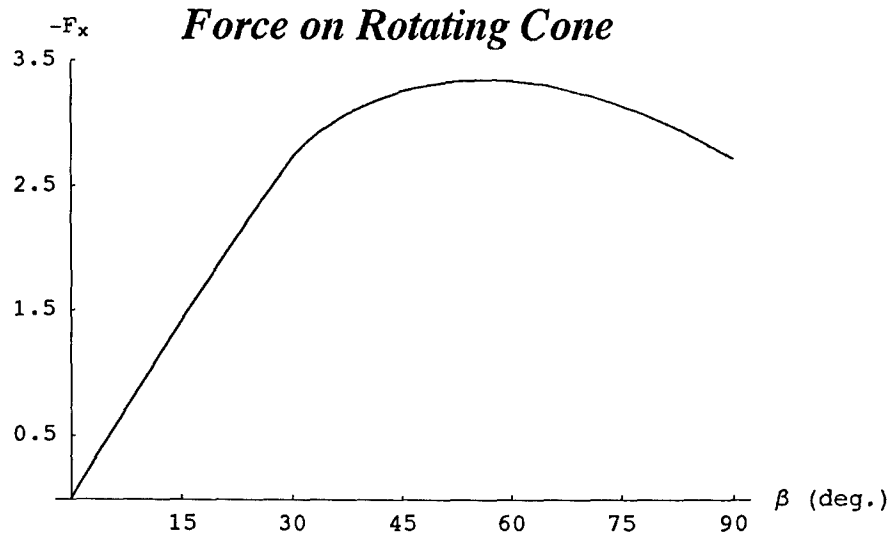

Figure 4.6. Spin Force on Cone in Hyperthermal Free-molecular Flow

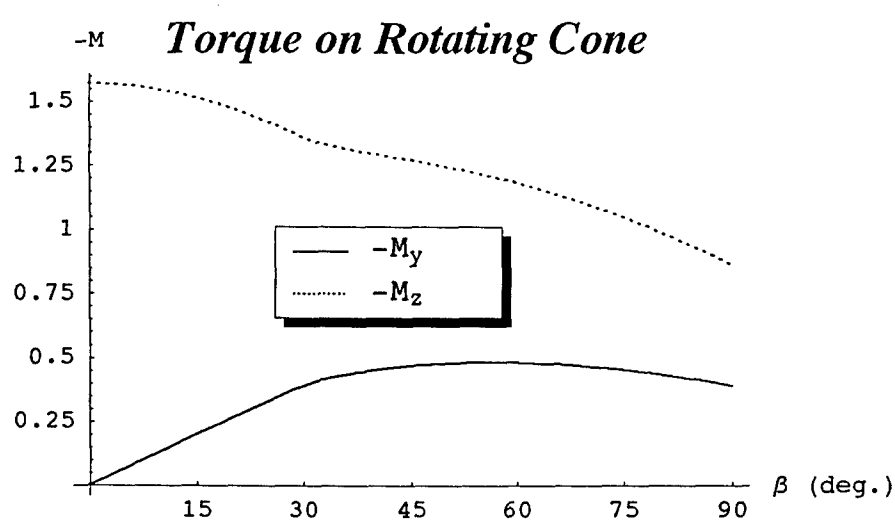

Figure 4.7. Spin Moments on Cone in Hyperthermal Free-molecular Flow

5. Rotating Axisymmetric Bodies in Free-molecular Flow

We proceed to generalize the analysis presented in the previous section for a body rotating about an axis of symmetry in a free molecular flow by removal of the hyperthermal assumption. General expressions in the form of surface integrals are obtained for the aerodynamic forces and moments which reduce to the previously obtained hyperthermal results in the case of an infinite molecular speed ratio. Again it is found that the body rotation gives rise to additional force and moment components proportional to the body's angular rate. Although quite intricate, closed form solutions are obtained for some simple body shapes and errors introduced by the hyperthermal assumption are investigated by examining the variations in the aerodynamic disturbances over a range of molecular speed ratios and angles of attack..

5.1 Mass and Momentum Flux

As depicted in Figure 4.1, an axisymmetric body rotates at angular rate ω about its axis of symmetry relative to the atmosphere We now suppose that a random velocity **u** described by the Maxwell-Boltzmann distribution is superimposed on the mean atmospheric flow. Define a spatially-fixed coordinate system $\{x,y,z\}$ with corresponding unit vectors **i**, **j**, **k** such that the z axis is along the axis of symmetry. The incident molecules have a *mean* velocity $\mathbf{V}_0$ relative to the origin O where $\mathbf{V}_0$ is at an angle β with respect to the $-z$ axis and is taken (without loss of generality) to lie in the y-z plane. The velocity **V** defined by $\mathbf{V}=\mathbf{V}_0-\boldsymbol{\omega}\times\mathbf{r}$, is the velocity of the incident molecules relative to the surface at position ***r*** *excluding* the random thermal motion of the atmosphere. The components of **V** along the local $\{\mathbf{n},\mathbf{b},\mathbf{t}\}$coordinate directions (see Sec. 4.1) are given respectively by

$$\begin{aligned} V_n &= V_0\left(\cos\beta\cos\theta+\sin\beta\sin\theta\cos\varphi\right)\\ V_b &= V_0\left(\sin\beta\cos\theta\cos\varphi-\cos\beta\sin\theta\right)\\ V_t &= V_0\sin\beta\sin\varphi-\omega\bar{\rho} \end{aligned} \tag{5.1}$$

The number of molecules per unit volume with random velocities between **u** and **u**+d**u** is given by eq.(3.1)

$$\frac{\rho}{mV_a^3\pi^{3/2}}\exp\left(-\frac{u^2}{V_a^2}\right)du_1\,du_2\,du_3$$

where ρ is the gas (atmospheric) density, m is the mass of a single gas molecule, and V_a is the most probable speed of the gas molecules. The random velocity **u** is with respect to the mean motion of the gas and hence the velocity ***v*** of the incident molecules relative to the surface *including* the random thermal motion is given by ***v***=**V**+**u**. Resolving velocities along the local $\{\mathbf{n},\mathbf{b},\mathbf{t}\}$coordinate directions, it follows that the number of molecules per unit volume with surface relative velocity between ***v*** and ***v***+d***v*** is given by $f\left(v_n,v_b,v_t\right)dv_n\,dv_b\,dv_t$ where

$$f\left(v_n,v_b v_t\right)=\frac{\rho}{\pi^{3/2}mV_a^3}\exp\left(-\frac{V\cdot V}{V_a^2}\right)\exp\left(\frac{2V\cdot v-v\cdot v}{V_a^2}\right) \tag{5.2}$$

Following the argument given in Sec. 3.1, the net mass flux δQ (mass delivered per unit time per unit surface area) from all incident molecules is given by

$$\delta Q = m\int_{-\infty}^{\infty}\int_{-\infty}^{\infty}\int_{0}^{\infty} v_n\, f(v_n, v_b, v_t)\, dv_n\, dv_b\, dv_t$$

which can be expressed in the form

$$\delta Q = \frac{\rho}{\pi^{3/2}V_a^3}\exp\left(-\frac{V\cdot V}{V_a^2}\right)\int_{-\infty}^{\infty}\exp\left(\frac{2V_t v_t - v_t^2}{V_a^2}\right)dv_t \int_{-\infty}^{\infty}\exp\left(\frac{2V_b v_b - v_b^2}{V_a^2}\right)dv_b \int_{0}^{\infty} v_n \exp\left(\frac{2V_n v_n - v_n^2}{V_a^2}\right)dv_n$$

Performing the integration, we obtain

$$\delta Q = \rho V_0\, \Gamma_1(S\eta)/S \tag{5.3}$$

where $S \equiv V_0/V_a$ (molecular speed ratio; $S = \infty$ in the hyperthermal limit), $\Gamma_1(x)$ is given by eq.(3.6), and η is defined in eq.(4.7). The incident momentum flux $\mathbf{p}_i$ due to all impinging molecules is given by the expression

$$\mathbf{p}_i = m\int_{-\infty}^{\infty}\int_{-\infty}^{\infty}\int_{0}^{\infty}(v_n\mathbf{n} + v_b\mathbf{b} + v_t\mathbf{t})v_n\, f(v_n, v_b, v_t)\, dv_n\, dv_b\, dv_t$$

Utilizing eq.(5.2) and denoting the components of $\mathbf{p}_i$ along the $\{\mathbf{n},\mathbf{b},\mathbf{t}\}$ coordinate directions by p_{ni}, p_{bi}, p_{ti} respectively, we find

$$p_{ni} = \frac{\rho}{\pi^{3/2}V_a^3}\exp\left(-\frac{V\cdot V}{V_a^2}\right)\int_{-\infty}^{\infty}\exp\left(\frac{2V_b v_b - v_b^2}{V_a^2}\right)dv_b \int_{-\infty}^{\infty}\exp\left(\frac{2V_t v_t - v_t^2}{V_a^2}\right)dv_t \int_{0}^{\infty} v_n^2 \exp\left(\frac{2V_n v_n - v_n^2}{V_a^2}\right)dv_n$$

$$p_{bi} = \frac{\rho}{\pi^{3/2}V_a^3}\exp\left(-\frac{\mathbf{V}\cdot\mathbf{V}}{V_a^2}\right)\int_{-\infty}^{\infty} v_b \exp\left(\frac{2V_b v_b - v_b^2}{V_a^2}\right)dv_b \int_{-\infty}^{\infty}\exp\left(\frac{2V_t v_t - v_t^2}{V_a^2}\right)dv_t \int_{0}^{\infty} v_n \exp\left(\frac{2V_n v_n - v_n^2}{V_a^2}\right)dv_n$$

$$p_{ti} = \frac{\rho}{\pi^{3/2}V_a^3}\exp\left(-\frac{\mathbf{V}\cdot\mathbf{V}}{V_a^2}\right)\int_{-\infty}^{\infty}\exp\left(\frac{2V_b v_b - v_b^2}{V_a^2}\right)dv_b \int_{-\infty}^{\infty} v_t \exp\left(\frac{2V_t v_t - v_t^2}{V_a^2}\right)dv_t \int_{0}^{\infty} v_n \exp\left(\frac{2V_n v_n - v_n^2}{V_a^2}\right)dv_n$$

Performing the integrations and simplifying, we obtain the following expressions for the components of the incident momentum flux.

$$\begin{aligned} p_{ni} &= \rho V_0^2\, \Gamma_2(S\eta)/S^2 \\ p_{bi} &= \rho V_0 V_b\, \Gamma_1(S\eta)/S \\ p_{ti} &= \rho V_0 V_t\, \Gamma_1(S\eta)/S \end{aligned} \tag{5.4}$$

where $\Gamma_2(x)$ is given by eq.(3.8).

We also require an expression for p_w – the normal component of momentum flux which would be carried away from the surface by diffusely reflected molecules *if* they were in thermal equilibrium with the surface. We can write $p_w = V_w\, \delta Q$ where V_w, given by eq.(2.2), is average normal velocity for this class of molecules. Invoking eq.(5.3), we obtain

$$p_w = \rho V_0 V_w\, \Gamma_1(S\eta)/S \tag{5.5}$$

5.2 Aerodynamic Forces & Moments

The force per unit area, $\boldsymbol{P}$, exerted by the molecules upon the surface is given by eq.(4.10) in conjunction with eqs.(5.4) & (5.5) above.

$$\begin{aligned} P_n &= (2-\sigma_n)\rho V_0^2\,\Gamma_2(S\eta)/S^2 + \sigma_n \rho V_0 V_w\,\Gamma_1(S\eta)/S \\ P_b &= \sigma_t \rho V_0 V_b\,\Gamma_1(S\eta)/S \\ P_t &= \sigma_t \rho V_0 V_t\,\Gamma_1(S\eta)/S \end{aligned} \tag{5.6}$$

The expressions for the net aerodynamic force and torque along the spatial axes in the present situation is given by eqs.(4.11) & (4.12) with $H(\eta)$ replaced by unity and are in a form suitable for numerical evaluation. We now proceed to expand these force and moment expressions so as to reveal in an explicit manner the effects of body rotation upon these aerodynamic disturbances. Considerable simplification in evaluation of the integrals can be realized by making the following observations.

1) $\overline{\rho}$ and θ are independent of φ
2) P_n, and P_b are even functions of φ
3) P_t is the sum of an odd and even function of φ

The region of integration is described by: $\{-\pi < \varphi < \pi;\, z_1 < z < z_2\}$ and the element of surface area is given by eq.(4.5). In light of the above observations, we can express the force components in the form

$$\begin{aligned} F_x &= -2\sigma_t \rho V_0\,\omega/S \int_{z_1}^{z_2}\int_0^{\pi} \overline{\rho}^2 \csc\theta\cos\varphi\,\Gamma_1(S\eta)\,d\varphi dz \\ F_y &= 2\rho V_0^2 \int_{z_1}^{z_2}\int_0^{\pi}\Big[\Big(\sigma_t \sin\beta\sin^2\varphi + \sigma_t\xi\cos\theta\cos\varphi + \sigma_n \frac{V_w}{V_0}\sin\theta\cos\varphi\Big)\Gamma_1(S\eta)/S + \\ &\qquad (2-\sigma_n)\sin\theta\cos\varphi\,\Gamma_2(S\eta)/S^2\Big]\overline{\rho}\csc\theta\,d\varphi dz \\ F_z &= 2\rho V_0^2 \int_{z_1}^{z_2}\int_0^{\pi}\Big[\Big(\sigma_t\xi\sin\theta - \sigma_n\frac{V_w}{V_0}\cos\theta\Big)\Gamma_1(S\eta)/S - (2-\sigma_n)\cos\theta\,\Gamma_2(S\eta)/S^2\Big]\overline{\rho}\csc\theta\,d\varphi dz \end{aligned} \tag{5.7}$$

where $\xi = \sin\beta\cos\theta\cos\varphi - \cos\beta\sin\theta$

The components of the aerodynamic moment about the origin of the spatial axes are given by

$$
\begin{aligned}
M_x = 2\rho V_0^2 \int_{z_1}^{z_2}\int_0^{\pi} \Big\{ & \Big[\sigma_n V_w/V_0\,(\bar{\rho}\cos\theta - z\sin\theta)\cos\varphi - \sigma_t(z\cos\theta + \bar{\rho}\sin\theta)\xi\cos\varphi \\
& - \sigma_t z\sin\beta\sin^2\varphi\Big]\Gamma_1(S\eta)/S + \\
& (2-\sigma_n)(\bar{\rho}\cos\theta - z\sin\theta)\cos\varphi\,\Gamma_2(S\eta)/S^2\Big\}\bar{\rho}\csc\theta\, d\varphi dz \\
M_y = -2\sigma_t\rho V_0\omega/S \int_{z_1}^{z_2}\int_0^{\pi} & z\bar{\rho}^2\csc\theta\cos\varphi\,\Gamma_1(S\eta)\,d\varphi dz \\
M_z = -2\sigma_t\rho V_0\omega/S \int_{z_1}^{z_2}\int_0^{\pi} & \bar{\rho}^3\csc\theta\,\Gamma_1(S\eta)\,d\varphi dz
\end{aligned}
\tag{5.8}
$$

As in the hyperthermal case, the body's rotation has no affect on F_y, F_z and M_x but introduces additional disturbances F_x, M_y and M_z proportional to the rotational rate. Additionally, we can again show that the lift force acts in the direction of $\boldsymbol{\omega}\times\mathbf{V}_0$; which according to Fig. 4.1, requires $F_x < 0$ for $\omega > 0$. Hence we must prove that (see eq.(5.7))

$$
\int_{z_1}^{z_2} \bar{\rho}^2\csc\theta \int_0^{\pi} \cos\varphi\,\Gamma_1(S\eta)d\varphi\, dz \geq 0
$$

Since $\theta, \beta \in (0,\pi)$, $\sin\theta \geq 0$ and $\sin\beta \geq 0$. It is therefore sufficient to demonstrate that the inner integral is nonnegative. From eq.(4.7) we can write $\eta = a\cos\varphi + b$; where $a = \sin\beta\sin\theta \geq 0$, and $b = \cos\beta\cos\theta$. It is easy to show that

$$
\int_0^{\pi} \cos\varphi\,\Gamma_1(S\eta)d\varphi = \int_0^{\pi/2} \left[\Gamma_1(Sb + Sa\cos\varphi) - \Gamma_1(Sb - Sa\cos\varphi)\right]\cos\varphi\, d\varphi
$$

Now the function $\Gamma_1(x)$ is an increasing function of x and $Sb + Sa\cos\varphi \geq Sb - Sa\cos\varphi$ for $0 \leq \varphi \leq \pi/2$. It follows that $\int_0^{\pi} \cos\varphi\,\Gamma_1(S\eta)\,d\varphi \geq 0$ *(QED)*

Recalling the two limits given by eqs.(3.14) & (3.15)

$$
\lim_{S\to\infty} \frac{\Gamma_1(S\eta)}{S} = \eta\, H(\eta), \qquad \lim_{S\to\infty} \frac{\Gamma_2(S\eta)}{S^2} = \eta^2\, H(\eta)
$$

where $H(x)$is the Heaviside step function, it is easy to show that the expressions (5.7) & (5.8) reduce respectively to the hyperthermal results obtained previously in eqs.(4.14) & (4.15).

5.3 Closed Form Solutions

Although the calculations are rather intricate, we will find closed form expressions for the aerodynamic forces and moments on a circular disk, sphere, right circular cylinder and right circular cone where each body rotates about its axis of symmetry. Since results for the non-rotating case have been provided in Sec. 3.2, we shall only consider disturbances arising from body rotation. It will be demonstrated that the resulting expressions reduce to those obtained in Sec.4.3 (hyperthermal assumption) as the molecular speed ratio tends to infinity.

5.3.1 Spinning Disk in Free-molecular Flow

We consider the disk $x^2+y^2 \le R^2$ lying in the plane z=0. Note that unlike the hyperthermal case, even if we restrict the angle of attack to $0 \le \beta \le \pi/2$ the disk experiences impingement on both the top and bottom surfaces due to the random thermal motion of the molecules. On the top surface $\theta = 0, \eta = \cos\beta$ while on the bottom surface $\theta = \pi, \eta = -\cos\beta$. Due to the degenerate nature of this surface, we need to modify the form of the integrals given in eqs.(5.7) & (5.8) by replacing the element of surface area $(\bar{\rho}\csc\theta\, d\varphi dz)$by $\bar{\rho}\, d\bar{\rho} d\varphi$ and integrating over the region $\{0 < \bar{\rho} < R; 0 < \varphi < \pi\}$. We find that both $F_x(\omega)$ and $M_y(\omega)$ vanish while the disk rotation produces a torque opposing the direction of spin given by

$$M_z(\omega) = -\frac{\pi}{2}\sigma_t \rho V_0 R^4 \omega \left[\Gamma_1(S\cos\beta) + \Gamma_1(-S\cos\beta)\right]/S \tag{5.9}$$

Now $\lim_{S\to\infty} M_z = -\pi/2\,\sigma_t \rho V_0 R^4 \omega \cos\beta$ in agreement with the hyperthermal result obtained in Sec. 4.3.1. At the other extreme, when S=0 $(V_a$ finite, $V_0 = 0)$ we have $M_z = -\sqrt{\pi}/2\,\sigma_t \rho V_a R^4 \omega$.

Figure 5.1 shows the variation of M_z (scaled by $-\pi\sigma_t \rho V_0 R^4 \omega/2$) with angle of attack for the two cases $S = 2$and $S = \infty$. It is observed that the hyperthermal approximation breaks down at high angles of attack; at $\beta = 90^\circ$ it yields zero torque while a nonzero value obtains under a finite molecular speed ratio.

In Figure 5.2, we have plotted the percentage error in M_z corresponding to the hyperthermal approximation as a function of S for several values of angle of attack. Again, the error increases with angle of attack and is 100% at $\beta = 90^\circ$.

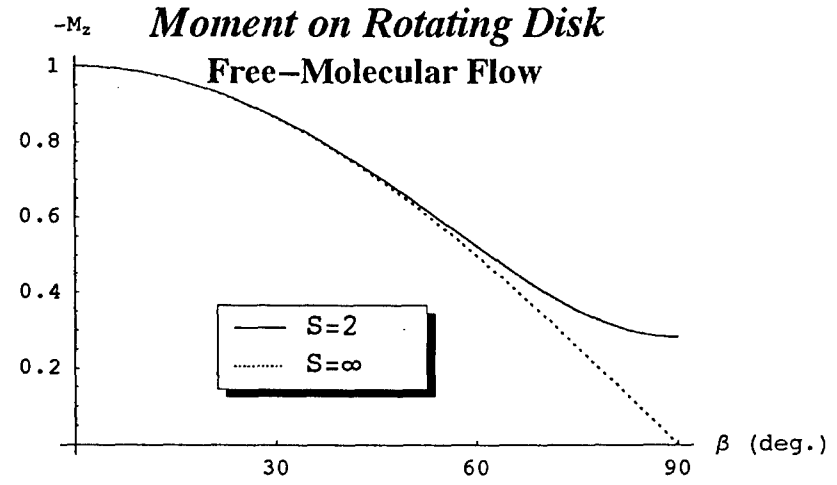

Figure 5.1. Spin Moment on Disk in Free-molecular Flow

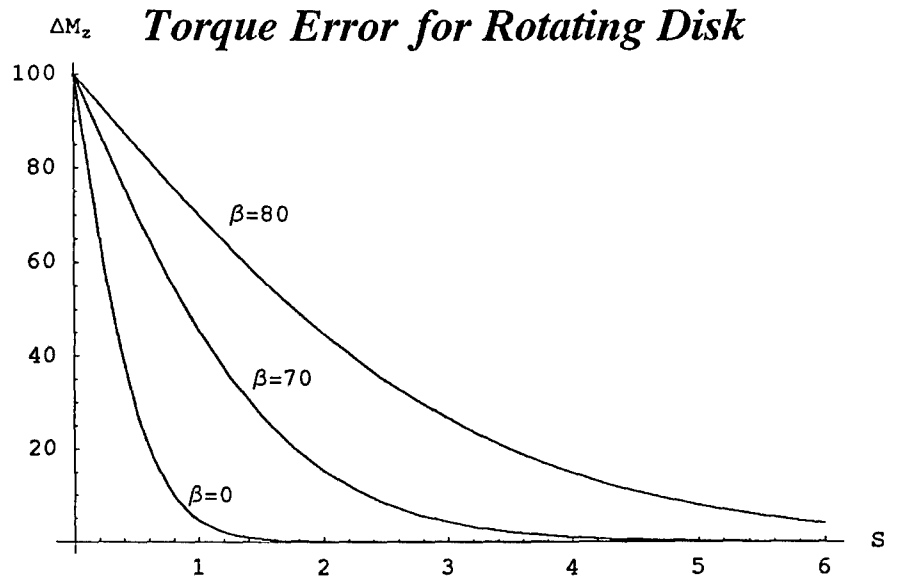

Figure 5.2. Disk Hyperthermal Spin Moment Error

5.3.2 Spinning Sphere in Free-molecular Flow

Consider a rotating sphere of radius R in a free molecular flow as shown in Fig.4.2. Following the procedure in Sec. 4.3.2, we rotate to a Cartesian frame $\{X, Y, Z\}$ so that the mean flow velocity V_0 is parallel to the $(-Z)$ axis and introduce a system of spherical coordinates $\{R,\Theta,\Phi\}$ defined by eqs.(4.16). The flow is symmetric with respect to the $\{Y, Z\}$ plane, hence the integrands in eqs.(5.7) & (5.8) are even functions of Φ. In the integrands, we set $\eta = \cos\Theta$, $\overline{\rho}\ \csc\theta\, d\varphi\, dz \to R^2 \sin\Theta\, d\Theta\, d\Phi$ and make use of eqs.(4.17) while first performing the integration over Φ (recall that due to the random thermal motion, we must integrate over the entire surface of the sphere).

The lift force $F_x(\omega)$ reduces to the definite integral

$$F_x = -2\pi\sigma_t \rho V_0 R^3 \omega S^{-1} \sin\beta \int_0^\pi \sin\Theta\cos\Theta\,\Gamma_1(S\cos\Theta)\,d\Theta$$

Making the substitution $x = S\cos\Theta$ and invoking eq.(3.16) we obtain

$$F_x = -2\pi/3\,\sigma_t \rho V_0 R^3 \omega \sin\beta \tag{5.10}$$

Interestingly, the lift force is independent of S and of course agrees with the hyperthermal result obtained in Sec. 4.3.2.

The expression for the moment $M_y(\omega)$ can be reduced to

$$M_y = -\pi\sigma_t \rho V_0 R^4 \omega S^{-1} \sin 2\beta \int_0^\pi \sin\Theta\left(\cos^2\Theta - 1/2\sin^2\Theta\right)\Gamma_1(S\cos\Theta)\,d\Theta$$

Performing the same substitution as above, we obtain the final expression

$$M_y = -\pi/8\,\sigma_t \rho V_0 R^4 \omega\, \mathcal{A}(S)\sin 2\beta \tag{5.11}$$

where

$$\mathcal{A}(S) = \frac{2S^2 - 3}{2\sqrt{\pi}S^3}\exp(-S^2) + \frac{4S^4 - 4S^2 + 3}{4S^4}\,\mathrm{erf}(S)$$

Since $\lim_{S\to 0}\mathcal{A}(S) = 0$ and $\lim_{S\to\infty}\mathcal{A}(S) = 1$, this component of the aerodynamic moment vanishes when the mean flow velocity is zero (with random thermal motion) and agrees with the result obtained previously under hyperthermal conditions.

Finally, the moment $M_z(\omega)$ can be reduced to the form

$$M_z = -\pi/4\,\sigma_t \rho V_0 R^4 \omega S^{-1} \int_0^\pi \left[5 - \cos 2\beta - (1 + 3\cos 2\beta)\cos 2\Theta\right]\sin\Theta\,\Gamma_1(S\cos\Theta)\,d\Theta$$

Performing the integration, we find

$$M_z = -\pi/8\,\sigma_t\, \rho V_0 R^4 \omega\left[\mathcal{B}(S) - \mathcal{A}(S)\cos 2\beta\right] \tag{5.12}$$

where

$$\mathcal{B}(S) = \frac{10S^2 + 1}{2\sqrt{\pi}S^3}\exp\left(-S^2\right) + \frac{20S^4 + 12S^2 - 1}{4S^4}\,\mathrm{erf}(S)$$

Since $\lim_{S\to\infty}\{\mathcal{A}(S),\mathcal{B}(S)\}=\{1,5\}$, we recover the hyperthermal limit as obtained in Sec. 4.3.2. To obtain the limiting value of M_z as S (V_0) approaches zero, we replace V_0 with SV_a and note that $\lim_{S\to 0}\{\mathcal{A}(S),S\mathcal{B}(S)\}=\left\{0,32/\left(3\sqrt{\pi}\right)\right\}$. Hence, under a zero mean flow the sphere experiences a nonzero moment when spinning in a Maxwellian atmosphere.

$$\lim_{S\to 0} M_z = -4\sqrt{\pi}/3\sigma_t\rho V_a R^4\omega$$

The functions $\mathcal{A}$(S) and $\mathcal{B}$(S) are plotted below in Fig. 5.3. Since $0<\mathcal{A}(S)<1$ for $0<S<\infty$, the magnitude of M_y is overestimated by the hyperthermal approximation. Figure 5.4 shows the variation of $|M_z|$ (scaled by $\pi/8\sigma_t\rho V_0 R^4\omega$) with angle of attack for the two cases S=5 and S=∞. In contrast to the rotating disk (Fig. 5.1), the torque magnitude increases with β and the difference between the two cases are approximately uniform over the full range of angle of attack.. The plots contained in Figure 5.5 show the percentage error in M_z based on the hyperthermal approximation as a function of S for selected values of the angle of attack (β). As opposed to the problem of the rotating disk (see Fig. 5.2), the error is not greatly influenced by the angle of attack and now *decreases* with increasing β.

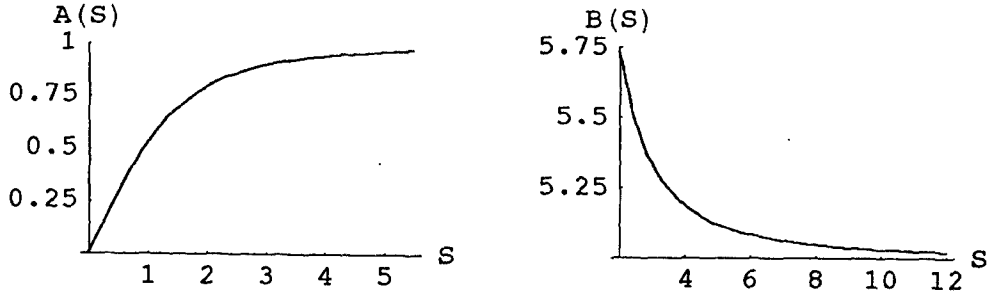

Figure 5.3. The Functions $\mathcal{A}$(S) & $\mathcal{B}$(S)

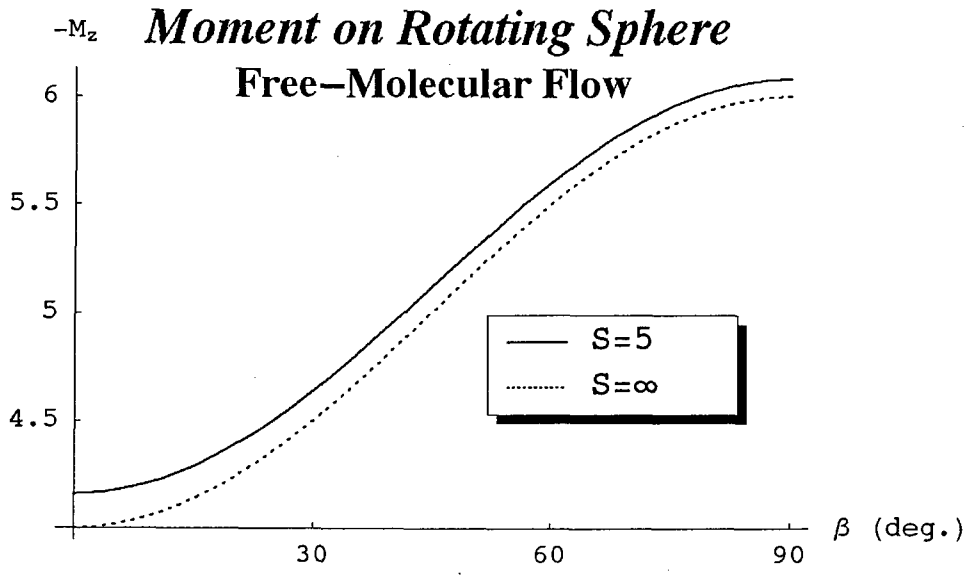

Figure 5.4. Spin Moment $M_z(\omega)$ on Sphere in Free-molecular Flow

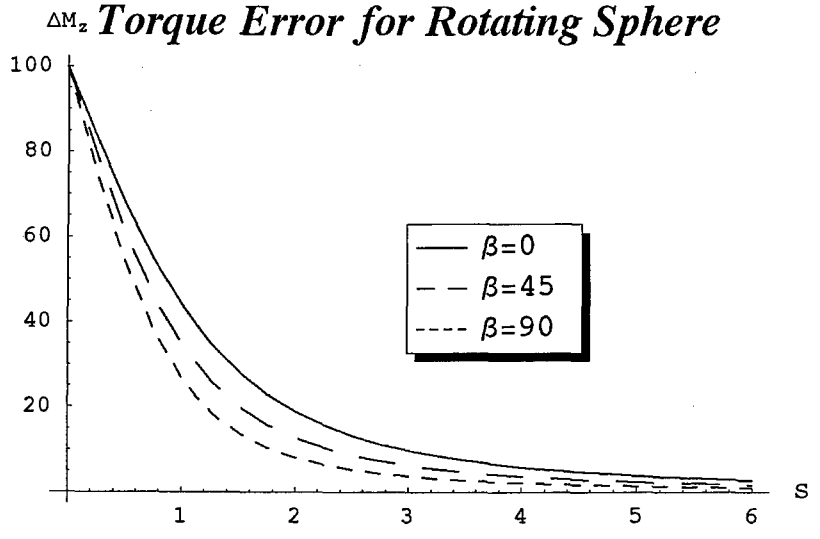

Figure 5.5. Sphere Hyperthermal Spin Moment Error

5.3.3 Spinning Cylinder in Free-molecular Flow

With reference to Fig. 4.1, a right circular cylinder of radius R and length L has its centroid at the origin of the Cartesian coordinate system $\{x, y, z\}$. The cylinder is rotating about its axis (z) at angular rate ω with an impinging free-molecular flow incident at angle of attack β with respect to the -z axis. Due to the random thermal motion of the molecules, impingement occurs on both the top and bottom faces of the cylinder in addition to its lateral surface. We will use the superscripts 'l', 't' & 'b' to distinguish forces/moments on the lateral, top and bottom surfaces respectively.

On the lateral surface we have $\bar{\rho} = R$, $\theta = \pi/2$ and $\eta = \sin\beta\cos\varphi$ (see eq.(4.7)). Computing the lift force from eq.(5.7) and performing the z integration, we obtain

$$F_x^l(\omega) = -2\sigma_t \rho V_0 R^2 L\omega S^{-1} \int_0^\pi \cos\varphi\, \Gamma_1(\mu\cos\varphi)\, d\varphi \qquad (\mu \equiv S\sin\beta)$$

The integral appearing in the above expression has been previously evaluated (see eq.(3.23)) and leads to the result

$$F_x^l(\omega) = -\frac{\pi}{2}\omega\sigma_t \rho V_0 R^2 L \sin\beta$$

As in the previous example of the sphere, the lift force is independent of S and agrees with the hyperthermal expression obtained in Sec. 4.3.3.

Calculating the moments on the lateral surface from eqs.(5.8) we find that $M_y^l(\omega)$ vanishes while $M_z^l(\omega)$ can be expressed in the form

$$M_z^l(\omega) = -2\sigma_t \rho V_0 R^3 L\omega S^{-1} \int_0^\pi \Gamma_1(\mu\cos\varphi)\, d\varphi$$

Appealing to eq.(3.20) for evaluation of the integral, we obtain

$$M_z^l(\omega) = -\sqrt{\pi}\,\sigma_t \rho V_0 R^3 L\omega S^{-1} e^{-\mu^2/2}\left[\left(\mu^2+1\right) I_0\left(\mu^2/2\right) + \mu^2 I_1\left(\mu^2/2\right)\right]$$

where $I_\nu(\,)$ denotes the modified Bessel function of the first kind of order ν. Exploiting the second limit following eq.(3.24), we recover the hyperthermal result obtained in Sec.4.3.3. At the other extreme, we easily can demonstrate that

$$\lim_{S\to 0} M_z^l(\omega) = -\sqrt{\pi}\,\sigma_t \rho V_a R^3 L\omega$$

On the top and bottom surfaces of the cylinder we have $\theta = 0, \eta = \cos\beta$ and $\theta = \pi, \eta = -\cos\beta$ respectively. Adopting the results obtained in Sec.5.3.1 for circular disk, we find:

On the top surface $F_x^t = M_y^t = 0$

$$M_z^t(\omega) = -\pi/2\,\sigma_t \rho V_0 R^4 \omega S^{-1} \Gamma_1(S\cos\beta)$$

On the bottom surface $F_x^b = M_y^b = 0$

$$M_z^b(\omega) = -\pi/2\,\sigma_t \rho V_0 R^4 \omega S^{-1} \Gamma_1(-S\cos\beta)$$

Adding the contributions from all three surfaces, we obtain the net aerodynamic force and torque (about the centroid of the cylinder) due to rotation.

$$F_x(\omega) = -\pi/2\,\sigma_t \rho V_0 \omega\, R^2 L \sin\beta$$

$$M_y(\omega) = 0 \tag{5.13}$$

$$M_z(\omega) = -\sigma_t \rho V_0 R^3 \omega\, S^{-1} \left\{ \frac{\pi}{2} R\left[\Gamma_1(S\cos\beta) + \Gamma_1(-S\cos\beta)\right] + \sqrt{\pi} L e^{-\mu^2/2}\left[\left(\mu^2+1\right) I_0\left(\mu^2/2\right) + \mu^2 I_1\left(\mu^2/2\right)\right] \right\}$$

For the purposes of numerical evaluation we take the cylinder dimensions to be R=1 and L=5.

Figure 5.6 shows the variation of $|M_z|$ (scaled by $\sigma_t \rho V_0 \omega$) with angle of attack for the two cases S=3 and $S = \infty$. It is seen that the error in the hyperthermal assumption is most pronounced at small angles of attack. The Plots Contained in Figure 5.7 show the percentage error in M_z based on the hyperthermal approximation as a function of S for a range of angles of attack between 0 and 90 degrees. Again, it is observed that the errors are largest at small angles of attack and are non-negligible even at S=8 for small β.

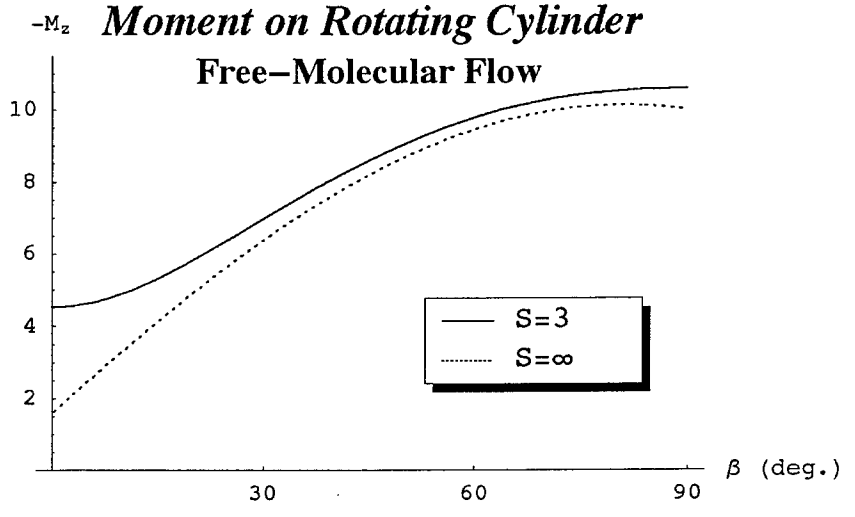

Figure 5.6. Spin Moment on Cylinder in Free-molecular Flow

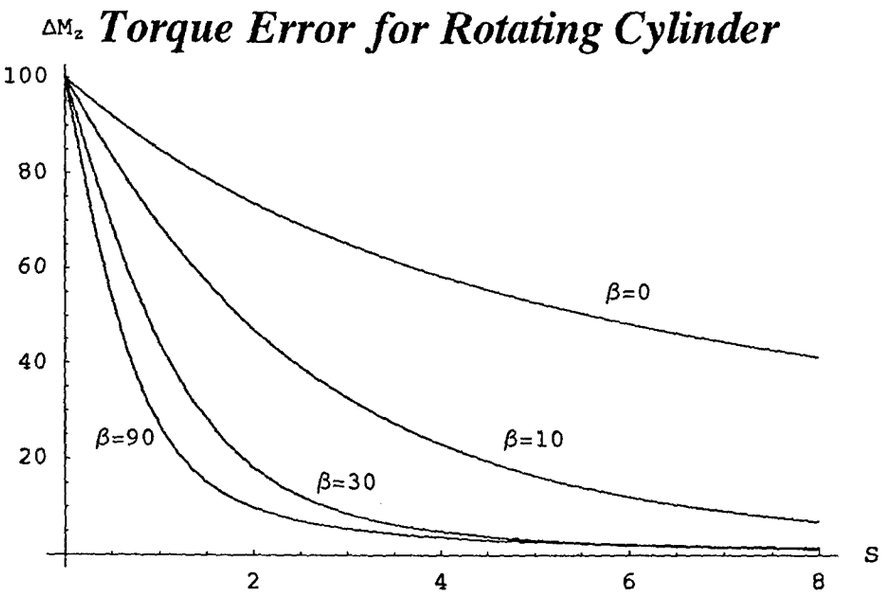

Figure 5.7. Cylinder Hyperthermal Spin Moment Error

5.3.4 Spinning Cone in Free-molecular Flow

We consider a right circular cone as shown in Fig. 4.5 in which a free molecular flow with mean velocity $\mathbf{V}_0$ is incident at angle β to its axis. The cone has base radius R and height L and is rotating at the angular rate ω about its axis. Due to the random thermal motion of the molecules, impingement occurs on the bottom surface of the cone in addition to its lateral surface for any value of β.

On the lateral surface: $\theta = \pi/2 - \gamma$, $\bar{\rho} = R(1 - z/L)$, and $\eta = \cos\beta\sin\gamma + \sin\beta\cos\gamma\cos\varphi$
where γ is the half-angle of the cone ($\tan\gamma = R/L$)

Computing the spin induced lift force and moments from eqs.(5.7)–(5.8) and performing the z integration, we obtain

$$F_x^l(\omega) = -\frac{2}{3}\sigma_t\rho V_0 R^3\omega\csc\gamma\ \frac{1}{S}\int_0^\pi \cos\varphi\,\Gamma_1(S\eta)\,d\varphi$$
$$M_y^l(\omega) = \frac{R}{4}\cot\gamma\ F_x^l(\omega)$$
$$M_z^l(\omega) = -\frac{1}{2}\sigma_t\rho V_0 R^4\omega\csc\gamma\ \frac{1}{S}\int_0^\pi \Gamma_1(S\eta)\,d\varphi$$

On the bottom surface of the cone, the force and moment calculation follows that performed in Sec. 5.3.1 with $\theta = \pi$ and $\eta = -\cos\beta$. Adding this contribution to the above yields the net aerodynamic force and moment (about the center of the base) due to rotation.

$$F_x(\omega) = -\frac{2}{3}\sigma_t\rho V_0 R^3\omega\csc\gamma\ \frac{1}{S}\int_0^\pi \cos\varphi\,\Gamma_1(S\eta)\,d\varphi$$
$$M_y(\omega) = \frac{R}{4}\cot\gamma\ F_x(\omega) \qquad (5.14)$$
$$M_z(\omega) = -\frac{\sigma_t\rho V_0 R^4\omega}{2S}\left\{\pi\Gamma_1(-S\cos\beta) + \csc\gamma\int_0^\pi \Gamma_1(S\eta)\,d\varphi\right\}$$

Utilizing the limit in eq.(3.14), we can show that these expressions simplify to the hyperthermal results obtained previously in Sec.4.3.4. In general, the integrals appearing in the above formulas must be evaluated numerically. We can however obtain closed form expressions for the special cases of longitudinal (β=0) and transverse $(\beta = \pi/2)$ flow.

When β=0, we readily find that $F_x(\omega) = M_y(\omega) = 0$ and

$$M_z(\omega) = -\frac{\pi}{2}\sigma_t\rho V_0 R^4\omega S^{-1}\left[\Gamma_1(-S) + \csc\gamma\,\Gamma_1(S\sin\gamma)\right]$$

When $\beta = \pi/2$, we can show that

$$F_x(\omega) = -\pi/6\,\sigma_t\rho V_0 R^3\omega\cot\gamma$$
$$M_y(\omega) = -\pi/24\,\sigma_t\rho V_0 R^4\omega\cot^2\gamma$$
$$M_z(\omega) = -\sqrt{\pi}/4\,\sigma_t\rho V_0 R^4\omega S^{-1}\left\{1 + \csc\gamma\exp\left(-\kappa^2/2\right)\left[\left(1+\kappa^2\right)I_0\left(\kappa^2/2\right) + \kappa^2 I_1\left(\kappa^2/2\right)\right]\right\}$$

where $\kappa = S\cos\gamma$ and $I_\nu(\ )$ denotes the modified Bessel function of the first kind of order ν. We note that for β=0 and $\pi/2$ both F_x and M_y are independent of S while M_z is a decreasing function of S.

The plots in Figure 5.8 show the relative error in $F_x(\omega)$ for the hyperthermal approximation for β=5, 50, & 70 degrees. It is observed that the error decreases with increasing angle of attack for a given molecular speed ratio. This is consistent with the fact established above that F_x is independent of S when β=90 degrees. Since the relation $M_y = R\cot\gamma\, F_x / 4$ holds both for finite S and in the hyperthermal limit, plots of the relative error in M_y are identical to those in Figure 5.8.

The relative error in the hyperthermal approximation to $M_z(\omega)$ is shown in Figure 5.9 for β=0, 45, & 90 degrees. In contrast with $M_y(F_x)$,the relative error now *increases* with increasing angle of attack for a given molecular speed ratio.

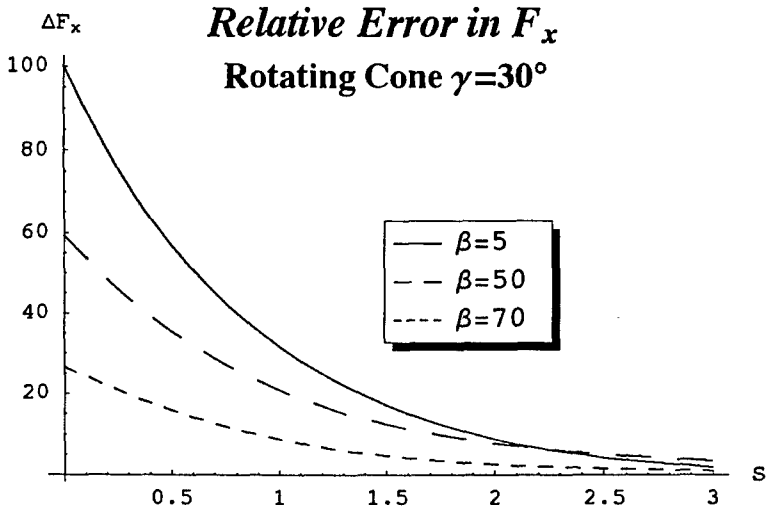

Figure 5.8. Cone Hyperthermal Spin Force Error

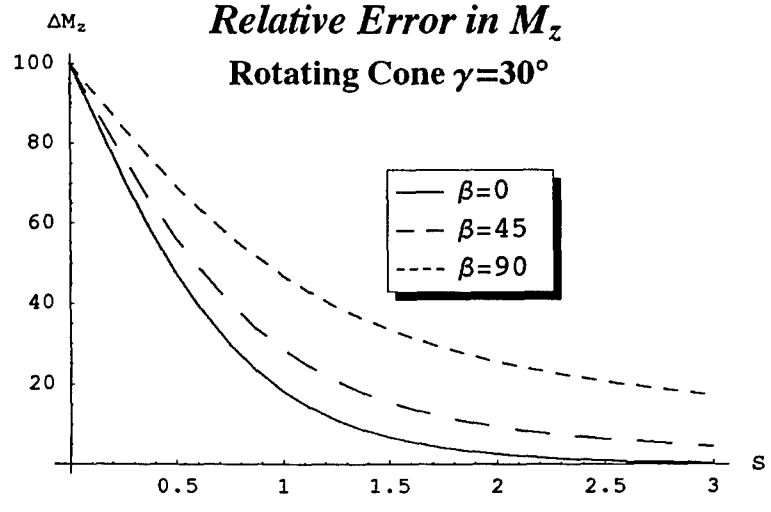

Figure 5.9. Cone Hyperthermal Spin Moment Error

References

[1] L.E. Wiggins, "Relative Magnitudes of the Space Environment Torques on a Satellite", *AIAA Journal*, Vol. 2, No. 4, pp. 770-771, 1964

[2] S.A. Schaaf and P.L. Chambre, *Flow of Rarefied Gases*, Princeton University Press, Princeton, N.J. , 1961

[3] M.W. Zemansky, *Heat and Thermodynamics*, 5th edition, McGraw-Hill.

[4] T.I. Gombossi, *Gaskinetic Theory*, Cambridge University Press, 1994.

Appendix: Elements of the Kinetic Theory of Gases

The purpose of this appendix is to present a concise account of those aspects of gas kinetic theory that are utilized in the report to calculate the aerodynamic disturbances on a body immersed in a free-molecular flow. We restrict our attention to ideal gases and develop the simple equation of state and the Maxwell-Boltzmannn velocity distribution from considerations of molecular collisions. Further details can be found in [3] & [4].

The Ideal Gas

It proves convenient to define an *ideal gas* by imposing the following assumptions which have been shown to be extremely reasonable in many areas of application.

1) The gas is composed of identical molecules which are separated by distances which are large compared with the molecular diameter. Any finite volume of gas contains an extremely large number of molecules. The first assumption will be valid for gases under low pressure. To appreciate the significance of the second assumption, we recall the experimental result that a 1 Kgm-mole of gas contains approximately 6.02214×10^{26} molecules (Avogadro's number). Since at standard conditions, 1 Kgm-mole of gas occupies a volume of 22.4 m^3, we see that there are approximately 3×10^{16} molecules in a cubic millimeter at standard conditions.

2) In the absence of external forces, the molecules are distributed uniformly throughout their container. Thus if their are a total of N molecules in a container of volume V, then the average number of molecules per unit volume, n, is $n = N/V$. It follows that a small volume element ΔV contains $n\Delta V$ molecules. Clearly, it is possible that by taking ΔV sufficiently small no molecules will be contained in the volume element. However, since the number density of molecules is so large, we can divide the container into extremely small elements of volume which still contain a large number of molecules. Even a cube 1/1000 mm on a side will contain approximately 3×10^7 molecules (at standard conditions). This dimension is infinitesimal compared with other physical dimensions of interest. We therefore are justified in applying the methods of differential and integral calculus to these "small" volume elements with negligible error. Thus the number of molecules in a differential volume element dV is given $n\,dV$.

3) Forces are exerted upon a molecule only when it collides with another molecule or the walls of its container; these collisions are regarded as perfectly elastic. The walls of the container are assumed to be smooth hence there will be no change in the tangential component of molecular velocity upon collision.

4) There is no preferred direction regarding the molecular velocity. Imagine a vector attached to each molecule with magnitude and direction scaled to its velocity. Transfer these vectors to a common origin and construct a sphere of arbitrary radius r centered at the origin. Our assumption implies that these vectors (prolonged if necessary) will intersect the sphere at a set of points uniformly distributed over its surface. The number of these points will be N, the number of molecules, and their surface density is given by $N/\left(4\pi r^2\right)$. Introducing spherical coordinates $\{r,\theta,\varphi\}$ at the center of the sphere where θ is the polar angle, we find that the number of molecules per unit volume with velocities having directions between $(\theta,\theta+d\theta)$ and $(\varphi,\varphi+d\varphi)$ is given by

$$dn_{\theta\varphi} = \frac{n}{4\pi}\sin\theta\, d\theta\, d\varphi \qquad \text{(A.1)}$$

5) Clearly, the speed of any given molecule changes continually due to collisions with other molecules or the walls of the container. To simplify the mathematics, we assume that the molecular speed can assume any value in the range $(0,\infty)$ and that the number of molecules with speeds in a specified range is constant for a gas in thermal equilibrium. Rigorously speaking, there will be a finite upper bound on the molecular speed. Later we will derive a statistical distribution of molecular speeds (based on these assumption) and show that this distribution function tails off very rapidly predicting a very small fraction of molecules with speeds in a high range. This provides justification for removing the finite upper bound on the molecular speed.

Molecular Surface Collisions

It is important to consider the number of molecular collisions per unit time per unit area of material surface. Figure A1 shows an element of surface area dA with normal **n** along with the polar and azimuth angles θ,φ. Molecules impinge upon the surface from all directions with all speeds. Let us consider only those molecules traveling with specific speed v and specific direction θ,φ which we term a "$\theta\varphi v$-molecule". More precisely, these molecules have speeds between v and $v+\Delta v$, and directions in the range $(\theta,\theta+d\theta)$ and $(\varphi,\varphi+d\varphi)$. In a time interval dt, the molecules which impinge on the surface are contained in a cylinder of slant height vdt and base area dA with corresponding volume $v\cos\theta\, dt\, dA$. If we denote by dn_v the number of molecules per unit volume with speeds between v and $v+dv$, then dn_v/n represents the fraction of molecules in this speed range. We make the further assumption that this fraction also applies to any subgroup of molecules e.g. those traveling in any particular direction. Utilizing eq.(A.1), we find that the number of $\theta\varphi v$-molecules per unit volume is given by

$$\frac{1}{4\pi}\sin\theta\, d\theta\, d\varphi\, dn_v$$

Thus the number of $\theta\varphi v$-molecules in the cylinder i.e. the number of collisions in time dt is

$$\frac{1}{4\pi}v\sin\theta\cos\theta\, d\theta\, d\varphi\, dn_v\, dA\, dt \qquad \text{(A.2)}$$

and the number impinging per unit time per unit area is given by

$$\frac{1}{4\pi}v\sin\theta\cos\theta\, d\theta\, d\varphi\, dn_v$$

By integrating the above expression over $\{0\le\theta\le\pi/2;\ 0\le\varphi\le 2\pi\}$, we obtain the number of molecules with speed v colliding with the surface from all directions per unit time per unit area

$$\frac{1}{4}v\, dn_v$$

In accordance with assumption (5) above, the total number of molecules impinging upon the surface per unit time per unit area is given by

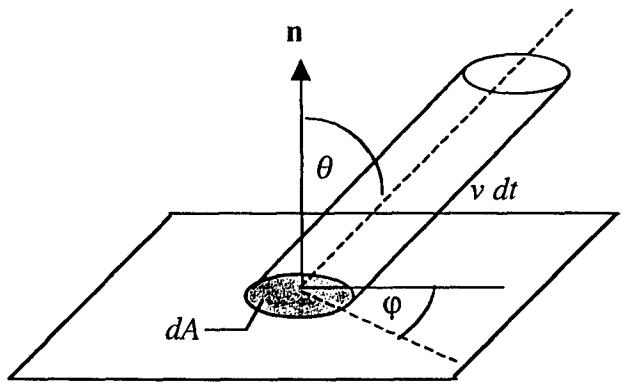

Figure A1 Molecule-Surface Collision

$$\frac{1}{4}\int_0^\infty v\,dn_v \tag{A.3}$$

We next relate the above integral to the average molecular speed. First consider the discrete case of N molecules for which N_1 have the same speed v_1, N_2 have the same speed v_2, etc. The average speed $\bar{v}$ is then given by

$$\bar{v} = \frac{N_1 v_1 + N_2 v_2 + \ldots}{N}$$

Dividing numerator and denominator by the volume V of the container, we can write

$$\bar{v} = \frac{n_1 v_1 + n_2 v_2 + \ldots}{n}$$

where n_i is the number of molecules per unit volume with speed v_i. Transitioning to the case of a continuous velocity distribution, we have

$$\bar{v} = \frac{1}{n}\int_0^\infty v\,dn_v$$

Utilizing this result in eq.(A.3) we arrive at the desired expression for the total number of molecules impinging upon the surface per unit time per unit area

$$\frac{1}{4} n \bar{v} \tag{A.4}$$

We now proceed to calculate the force imparted by the impinging molecules upon the surface. With reference to Fig. A1, consider a single $\theta\varphi v$ molecule of mass m before and after a surface collision. Regarding the material surface to be of infinite mass relative to the molecules, and recalling assumption (3) above, we find the change in momentum per molecular collision to be $2mv\cos\theta\,\mathbf{n}$. Multiplying by (A.2), we obtain the change in momentum $d\boldsymbol{p}$ for all $\theta\varphi v$ molecules colliding with the surface in the time interval dt.

$$d\boldsymbol{p} = \frac{1}{2\pi} m v^2 \sin\theta\cos^2\theta\; d\theta\, d\varphi\, dn_v\, dA\, dt\, \mathbf{n}$$

Integrating this result over the region $\{0 \le \theta \le \pi/2,\ 0 \le \varphi \le 2\pi,\ 0 \le v < \infty\}$ and dividing by dt gives the average force exerted by the surface on all the incident molecules. By Newton's third law, the force exerted by the molecules on the surface are oppositely directed with an associated pressure p given by the expression

$$p = \frac{1}{3} m \int_0^\infty v^2 dn_v$$

Following the same argument as given above for the average speed, we can express this integral in terms of $\overline{v^2}$ – the average value of the square of the speed.

$$p = \frac{1}{3} nm\overline{v^2} = \frac{1}{3} \rho \overline{v^2} \qquad \text{(A.5)}$$

where ρ denotes the gas density.

The above relation can be used to arrive at a molecular interpretation of absolute temperature. The equation of state of an ideal gas can be expressed in the form

$$pV = n\mathcal{R}T$$

where n is the number of moles, $\mathcal{R}$ is the Universal Gas Constant $\left(8314.5 \text{ joules / Kg-mole } ^\circ\text{K}\right)$, and T is the absolute temperature. But the number of moles is equal to the total number of molecules, N, divided by the number of molecules per mole, N_0–Avogadro's number $\left(6.02214 \times 10^{26} \text{ molecules / Kg-mole}\right)$. The universal constant $\mathcal{R}/N_0 \equiv k$ is Boltzmann's constant $\left(1.38065 \times 10^{-23} \text{ joules/molecule } ^\circ\text{K}\right)$, in terms of which the ideal gas law assumes the form

$$pV = NkT \qquad \text{(A.6)}$$

Since n is the number of molecules per unit volume, N/V, eq.(A.5) can be expressed in the form

$$pV = \frac{1}{3} Nm\overline{v^2}$$

If this is to agree with eq.(A.6), we must conclude that

$$\frac{1}{2} m\overline{v^2} = \frac{3}{2} kT \qquad \text{(A.7)}$$

which says that the mean translational kinetic energy of a gas molecule is proportional to the absolute temperature.

Distribution of Molecular Velocities

In this section we derive the celebrated Maxwell-Boltzmann velocity and speed distributions for an ideal gas. A rigorous derivation requires methods from statistical mechanics which will not be attempted here. We present essentially the argument originally given by Maxwell which although heuristic, is plausible from a physical point of view. In the previous section we arrived at expressions for the molecular flux and pressure in terms of the mean and rms molecular speeds respectively. By imposing additional assumptions, we can calculate the actual velocity *distribution* which will ultimately lead to relations between these average velocities and the gas temperature.

Consider a rectangular coordinate system whose axes $\{v_x, v_y, v_z\}$ correspond to the three components of molecular velocity. Each molecule in physical space has a corresponding point in this "velocity space". Since the number of molecules if finite, the distribution of these points in the velocity space will not be continuous. However, in view of assumptions (1) & (2) above, we will approximate this distribution by a continuous function with the understanding that any designated "volume element" in the velocity space must be chosen large enough so that it contains a large number of representative points. We start by posing the question: how many molecules (out of the total number N) have x components of velocity between v_x and v_x+dv_x ? This is equivalent to finding the number of points in velocity space contained in the thin slice parallel to the v_y-v_z plane between v_x and v_x+dv_x. If we denote this number by dN_{v_x}, then the fraction of the total number of molecules with x components of velocity between v_x and v_x+dv_x (regardless of there y or z velocity components) is dN_{v_x}/N. This fraction is certainly a function of v_x. It seems plausible that it should also be proportional to the thickness of the slice. Hence we write

$$\frac{dN_{v_x}}{N} = f(v_x)dv_x \tag{A.8}$$

where the function f is to be determined. By assumption (4) the velocity distribution is isotropic, so we must have for the same function f

$$\begin{aligned} \frac{dN_{v_y}}{N} &= f(v_y)dv_y \\ \frac{dN_{v_z}}{N} &= f(v_z)dv_z \end{aligned} \tag{A.9}$$

where dN_{v_y} and dN_{v_z} are defined analogously to dN_{v_x} We now impose the additional assumption that these fractions are also applicable to any subgroup of molecules e.g. for the subgroup of molecules with x components of velocity between v_x and v_x+dv_x $f(v_y)dv_y$ of them will also have a y component of velocity between v_y and v_y+dv_y. Thus the number of molecules simultaneously having x components of velocity between v_x and v_x+dv_x, y components between v_y and v_y+dv_y and z components between v_z and v_z+dv_z is given by

$$dN_{v_x v_y v_z} = N f(v_x) f(v_y) f(v_z) dv_x dv_y dv_z$$

Geometrically, this gives the number of representative points in the volume element $dv_x dv_y dv_z$ at the location (v_x, v_y, v_z) in velocity space. The number of representative points per unit volume then defines a "density" ρ

$$\rho = N f(v_x) f(v_y) f(v_z) \tag{A.10}$$

The change in ρ for small increments in v_x, v_y and v_z is given by

$$d\rho = \frac{\partial \rho}{\partial v_x} dv_x + \frac{\partial \rho}{\partial v_y} dv_y + \frac{\partial \rho}{\partial v_z} dv_z$$

Since the velocity distribution is isotropic, there will be no change in ρ if we restrict ourselves to those points that are at a fixed distance from the origin in velocity space i.e. $d\rho = 0$ under the constraint $v_x^2 + v_y^2 + v_z^2 = \text{const}$. Using eq.(A.10), this results can be expressed in the form

$$\frac{f'(v_x)}{f(v_x)} dv_x + \frac{f'(v_y)}{f(v_y)} dv_y + \frac{f'(v_z)}{f(v_z)} dv_z = 0 \tag{A.11}$$

for velocity increments satisfying

$$v_x dv_x + v_y dv_y + v_z dv_z = 0 \tag{A.12}$$

In eq.(A.11) only two of the differentials are independent. Utilizing eq.(A.12) we can recast eq.(A.11) in the form

$$\left[\frac{f'(v_x)}{f(v_x)} - \frac{f'(v_z)}{f(v_z)} \frac{v_x}{v_z} \right] dv_x + \left[\frac{f'(v_y)}{f(v_y)} - \frac{f'(v_z)}{f(v_z)} \frac{v_y}{v_z} \right] dv_y = 0$$

from which it follows that

$$\frac{f'(v_x)}{v_x f(v_x)} = \frac{f'(v_y)}{v_y f(v_y)} = \frac{f'(v_z)}{v_z f(v_z)}$$

The first ratio is a function only of v_x, while the second and third are respectively functions only of v_y and v_z. It follows that each is equal to a constant

$$\frac{f'(v_x)}{v_x f(v_x)} = -\lambda \qquad \text{etc.}$$

Integrating this equation and observing that $f(v_x) \to 0$ as $|v_x| \to \infty$, we obtain

$$f(v_x) = \alpha \exp(-\beta^2 v_x^2) \tag{A.13}$$

$(\beta^2 \equiv \lambda/2)$

Thus we have obtained the desired form of the velocity distribution function *f*. In the next section we will obtain the physical interpretation of the parameters α and β. We can now express the number of molecules with *x* components of velocity between v_x and $v_x + dv_x$ in the form (see eq.(A.8))

$$dN_{v_x} = N\alpha \exp(-\beta^2 v_x^2) dv_x \quad (-\infty < v_x < \infty)$$

(with similar expressions for dN_{v_y} and dN_{v_z}) and the number of points per unit volume (A.10) as

$$\rho = N\alpha^3 \exp\left(-\beta^2 v^2\right) \tag{A.14}$$

where v is the molecular speed.

Many times we are interested in the number of molecules with *speeds* in a certain range without regard to direction. The speed range of interest may be of finite or infinite length. Let us first find the number of molecules with speeds in the infinitesimal range between v and $v+dv$. Denoting this number by dN_v, we simply need to find the number of representative points inside the thin spherical shell of radius v and thickness dv in velocity space. Since ρ is uniform in this region, we simply multiply the density given in eq.(A.14) by the volume $4\pi v^2 dv$ of the shell

$$dN_v = 4\pi N\alpha^3 v^2 \exp\left(-\beta^2 v^2\right) dv \tag{A.15}$$

Note that the *velocity* distribution (A.14) assumes its maximum value at v=0 and decays exponentially to zero, while the speed distribution (A.15) is zero at v=0. increases to its maximum value and then decays exponentially to zero. The number of molecules with velocities in a desired range or having speeds in a specified interval can be calculated by integrating the appropriate distribution over the appropriate domain. Thus the number of molecules with speeds between v_1 and v_2 $\left(0 < v_1 < v_2\right)$ is obtained by integrating (A.15) over the interval $v_1 \le v \le v_2$.

Evaluation of the Distribution Parameters

We now show how the two velocity distribution parameters α and β can be related to the absolute temperature of the gas. Firstly, the integral of (A.15) over all speeds from zero to infinity must yield N–the total number of molecules. Performing the integration, we find that

$$\alpha = \beta/\sqrt{\pi}$$

The speed distribution (A.15) can then be expressed in terms of the single parameter β

$$dN_v = \frac{4N}{\sqrt{\pi}} \beta^3 v^2 \exp\left(-\beta^2 v^2\right) dv$$

We now relate the parameter β to the most probable, mean, and rms speeds. We define the most probable speed v_a to the value of v for which dN_v/dv assumes its maximum value. It is easy to show that

$$v_a = \beta^{-1}. \tag{A.16}$$

The mean speed $\bar{v}$ is given by

$$\bar{v} = \frac{1}{N}\int_0^\infty v\, dN_v = \frac{2}{\sqrt{\pi}\beta} \tag{A.17}$$

The rms speed is defined by

$$v_{\text{rms}}^2 = \frac{1}{N}\int_0^\infty v^2\, dN_v = \frac{3}{2\beta^2}$$

Combining this last relation with eq.(A.7), we deduce that

$$\beta = \sqrt{m/2kT} \tag{A.18}$$

allowing us to express all the distribution functions in terms of absolute temperature and molecular mass.

$$dN_v = \frac{4N}{\sqrt{\pi}}\left(\frac{m}{2kT}\right)^{3/2} v^2 \exp\left(-\frac{mv^2}{2kT}\right)dv$$

$$dN_{v_x v_y v_z} = \frac{N}{\pi^{3/2}}\left(\frac{m}{2kT}\right)^{3/2} \exp\left(-\frac{mv^2}{2kT}\right)dv_x\, dv_y\, dv_z \qquad \text{(A.19)}$$

$$dN_{v_x} = \frac{N}{\sqrt{\pi}}\left(\frac{m}{2kT}\right)^{1/2} \exp\left(-\frac{mv_x^2}{2kT}\right)dv_x$$

with corresponding expressions for dN_{v_y} and dN_{v_z}. Figure A2 shows the velocity distribution dN_v/dv for three different temperatures $T_1 < T_2 < T_3$. The area under the curves are all equal since this represents the number of gas molecules.

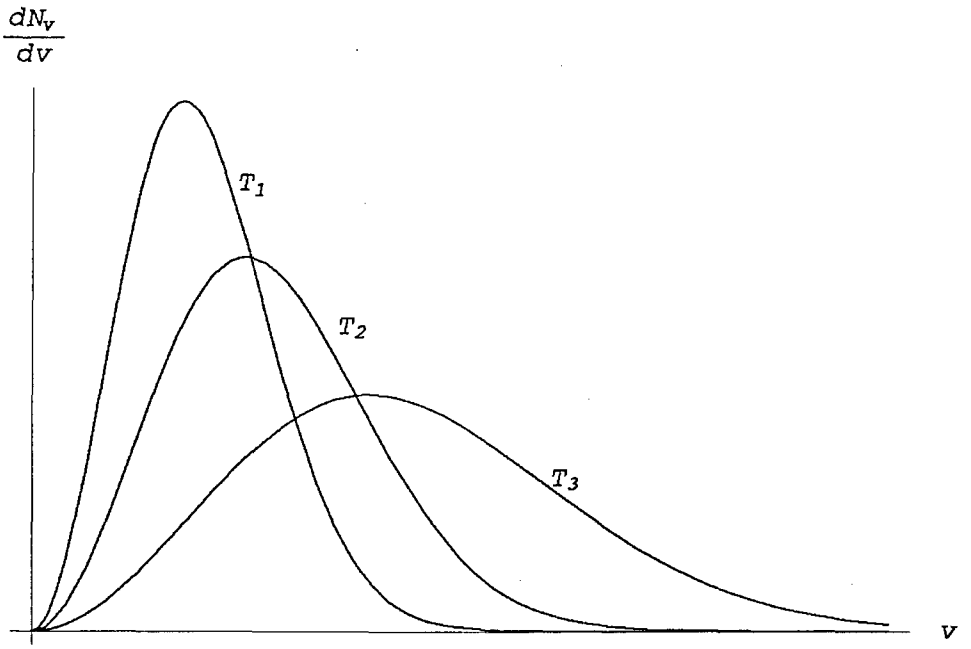

Figure A2 Speed Distribution Function